AD-A113 837 NAVAL POSTGRADUATE SCHOOL MONTEREY CA F/G 8/10
ONE-DIMENSIONAL MODEL PREDICTIONS OF UPPER OCEAN TEMPERATURE CH--ETC(U)
DEC 81 E F STEINER

UNCLASSIFIED NL

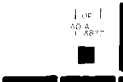

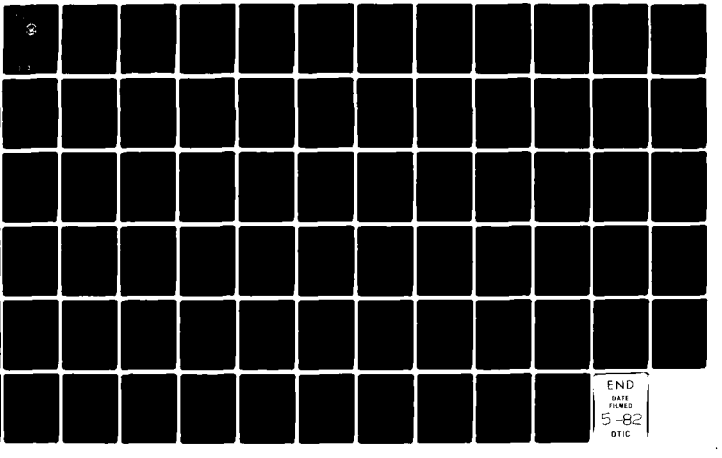

END
DATE FILMED
5-82
DTIC

(2)

NAVAL POSTGRADUATE SCHOOL
Monterey, California

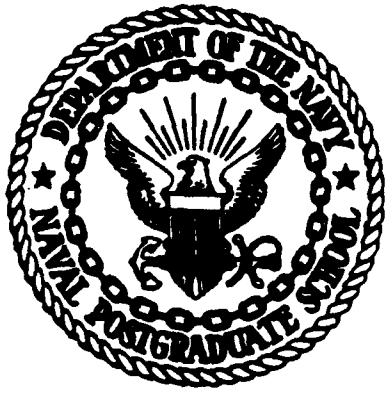

THESIS

ONE-DIMENSIONAL MODEL PREDICTIONS OF UPPER OCEAN TEMPERATURE CHANGES BETWEEN SAN FRANCISCO AND HAWAII

by

Edward F. Steiner

December 1981

Thesis Advisor: R.L. Elsberry

Approved for public release; distribution unlimited

UNCLASSIFIED

SECURITY CLASSIFICATION OF THIS PAGE (When Data Entered)

REPORT DOCUMENTATION PAGE	READ INSTRUCTIONS BEFORE COMPLETING FORM
1. REPORT NUMBER	2. GOVT ACCESSION NO. AD-A113837	3. RECIPIENT'S CATALOG NUMBER
4. TITLE (and Subtitle) One-Dimensional Model Predictions of Upper Ocean Temperature Changes Between San Francisco and Hawaii	5. TYPE OF REPORT & PERIOD COVERED Master's Thesis: December 1981
	6. PERFORMING ORG. REPORT NUMBER
7. AUTHOR(s) Edward F. Steiner	8. CONTRACT OR GRANT NUMBER(s)
9. PERFORMING ORGANIZATION NAME AND ADDRESS Naval Postgraduate School Monterey, California 93940	10. PROGRAM ELEMENT, PROJECT, TASK AREA & WORK UNIT NUMBERS
11. CONTROLLING OFFICE NAME AND ADDRESS Naval Postgraduate School Monterey, California 93940	12. REPORT DATE December 1981
	13. NUMBER OF PAGES 79
14. MONITORING AGENCY NAME & ADDRESS(if different from Controlling Office)	15. SECURITY CLASS. (of this report) Unclassified
	15a. DECLASSIFICATION/DOWNGRADING SCHEDULE

16. DISTRIBUTION STATEMENT (of this Report)

Approved for public release; distribution unlimited.

17. DISTRIBUTION STATEMENT (of the abstract entered in Block 20, if different from Report)

18. SUPPLEMENTARY NOTES

19. KEY WORDS (Continue on reverse side if necessary and identify by block number)

1 - D ocean modeling, oceanic heat budget, upper ocean prediction, atmospheric forcing

20. ABSTRACT (Continue on reverse side if necessary and identify by block number)

Previous tests of one-dimensional oceanic mixed layer models have generally used long time series of data at specific locations, such as at the ocean weather ships. In this work the Garwood model was used to make a series of predictions of upper ocean thermal structure changes along the shipping track between San Francisco and Hawaii, from 1 January to 16 December 1978. The initial and verifying ocean temperature profiles provided by the National Marine Fisheries Service, were objectively analyzed on a space-time grid, where the spatial dimension was along the shipping track. The grid resolution is

DD FORM 1 JAN 73 1473 EDITION OF 1 NOV 65 IS OBSOLETE S/N 0102-014-6601

UNCLASSIFIED

SECURITY CLASSIFICATION OF THIS PAGE (When Data Entered)

100 km and 15 days, which defines the basic prediction increment. The ocean mixed layer model was driven with the winds and heat fluxes derived from the Fleet Numerical Oceanography Center's atmospheric analyses. A preliminary check of local heat balance was made by comparing the observed change in heat content with the accumulated surface heat flux. Comparison of the observations and the 1-d mixed layer model predictions shows a large variability in model performance. Relatively good predictions were made during periods of shallowing or unchanging mixed layer depth, while poorer predictions occur during periods of rapid deepening. Variability along the track indicates superior performance in the subtropical region, with prediction accuracy decreasing in the region of the subtropical front and the California Current, where physical processes not included in the model are relatively large.

Approved for public release; distribution unlimited

One-Dimensional Model Predictions of Upper Ocean Temperature Changes Between San Francisco and Hawaii

by

Edward F. Steiner
Lieutenant, United States Navy
B.S., United States Naval Academy, 1974

Submitted in partial fulfillment of the
requirements for the degree of

MASTER OF SCIENCE IN METEOROLOGY AND OCEANOGRAPHY

from the

NAVAL POSTGRADUATE SCHOOL
December 1981

Author: Edward F. Steiner

Approved by: _____
Thesis Advisor

_____
Second Reader

_____
Chairman, Department of Meteorology

_____
Dean of Science and Engineering

ABSTRACT

Previous tests of one-dimensional oceanic mixed layer models have generally used long time series of data at specific locations, such as at the ocean weather ships. In this work the Garwood model was used to make a series of predictions of upper ocean thermal structure changes along the shipping track between San Francisco and Hawaii, from 1 January to 16 December 1978. The initial and verifying ocean temperature profiles provided by the National Marine Fisheries Service, were objectively analyzed on a space-time grid, where the spatial dimension was along the shipping track. The grid resolution is 100 km and 15 days, which defines the basic prediction increment. The ocean mixed layer model was driven with the winds and heat fluxes derived from the Fleet Numerical Oceanography Center's atmospheric analyses. A preliminary check of local heat balance was made by comparing the observed change in heat content with the accumulated surface heat flux. Comparison of the observations and the 1-d mixed layer model predictions shows a large variability in model performance. Relatively good predictions were made during periods of shallowing or unchanging mixed layer depth, while poorer predictions occur during periods of rapid deepening. Variability along the track indicates superior performance in the subtropical region, with prediction accuracy decreasing in the region of the subtropical front and the California Current, where physical processes not included in the model are relatively large.

TABLE OF CONTENTS

LIST OF TABLES

LIST OF FIGURES

ACKNOWLEDGEMENTS

The author wishes to thank Dr. Douglas R. McLain of the National Marine Fisheries Service for providing oceanic data; and Mr. Pat Gallacher of the Naval Postgraduate School for providing and interpolating FNOC atmospheric forcing fields, and for his valuable comments and assistance during the study. Appreciation is also due to Professor Bill Garwood for providing the ocean mixed layer prediction model and for his review of the thesis. The computing was done at the W. R. Church Computer Center.

The author wishes to express his sincerest appreciation to Professor R. L. Elsberry for the time and effort he has spent assisting in the defining and analysis of this study, and in the preparation of this manuscript.

I. INTRODUCTION

A. OCEANIC MIXED LAYER HYPOTHESIS AND BACKGROUND

The purpose of the study is to test the applicability of the Garwood (1977) one-dimensional mixed layer prediction model at a series of gridpoints along the shipping track between San Francisco and Hawaii. This spatial arrangement ensured model testing over a variety of oceanic regimes. Knowledge of the evolution of the mixed layer is an important requirement in the understanding of changing underwater sound propagation modes. This, in turn, is essential to the efficient operation of the U.S. Navy's submarine and antisubmarine warfare specialties. This study can illustrate the feasibility of using a one-dimensional model which does not include advective effects, in comparison to other prediction methods, such as persistence and climatology.

The Garwood model essentially treats heat and momentum fluxes at the ocean surface as primary factors in the modification of upper-ocean temperature profiles. The assumption of a local heat balance is made over proper time and space scales such that the change in heat content in the upper ocean is due solely to surface heat and momentum exchange. This means that other physical processes such as horizontal advection and diffusion are considered to be small relative to the effects at the surface. This basic concept describes the theory developed by Kraus and Turner (1967), which has been modified in subsequent research to include more accurate parameterizations of the physical processes involved.

The annual cycle of changes in the mixed layer is highly dependent on location. Factors which are important in this cycle include the

effects of annually changing radiation amounts, seasonal wind speed fluctuations, diurnal radiation and windspeed changes, and synoptic-scale storm events. Daytime heating causes shallowing of the oceanic mixed layer and the associated warming of the mixed layer. Nighttime upward heat flux tends to break down the shallow mixed layers built up during the day, with the associated cooling of the mixed layer. Larger windspeed values increase the amount of vertical mixing, which will also deepen the mixed layer. This diurnal pattern of changing mixed layer depths is superposed on the depth changes associated with the annual cycle of radiation changes. Strong winds, combined with relatively low insolation values during the winter, cause mixed layer depths to be relatively deep and mixed layer temperatures to be relatively low. This condition changes rapidly during the latter part of winter, when increasing amounts of solar radiation shallow the mixed layer on a daily basis. The reduction of the average windspeed during this same period, specifically due to the reduced frequency of winter storms, ensures that the mixed layer will shallow substantially for the duration of the summer months. A gradual warming of the mixed layer is also occurring throughout this period. Diurnal modification of the mixed layer depth is not as dramatic during this time period. The reduction of solar insolation in the fall, combined with the increasing frequency of winter storms, tend to increase mixed layer depths. A period of steadily increasing mixed layer depths, steadily decreasing mixed layer temperatures, and larger diurnal variations in mixed layer depth return with the change to winter conditions. The synoptic scale

storm frequency again becomes most critical in the maintenance of deep winter mixed layer depths.

B. STUDY DESCRIPTION

The study used a one-year time grid of 24 equal periods with a time interval of approximately 15 days. This time interval was chosen because it approximated the observed frequency of ship transit and data collection. The year 1978 was selected for the study as one with sufficiently complete atmospheric forcing and ocean temperature data, and one containing periods of significant ocean temperature changes.

The area selected is along a great circle track from San Francisco to Hawaii, approximately 1750 n mi in length (Fig. 1). A spatial grid of 33 points was created along this track, with a space interval of approximately 100 km. This space interval was chosen because it corresponds to the approximate distance between ship-launched expendable bathythermograph buoy data collection points. Two distinct oceanic regimes are contained in this area (Fig. 2). The northeastern portion of the track is under the influence of the California Current. The southwestern portion is under the influence of the relatively weak North Equatorial Current and is essentially in the calm area of the North Pacific oceanic gyre. The area between these two regimes contains the semi-permanent Subtropical Front which has its maximum density gradients in April. Interaction of the California Current with the homogeneous water mass to the south can be observed over a much broader region than the Subtropical Front, which merely marks the location of the strongest gradients in temperature and salinity. The relative accuracy of the

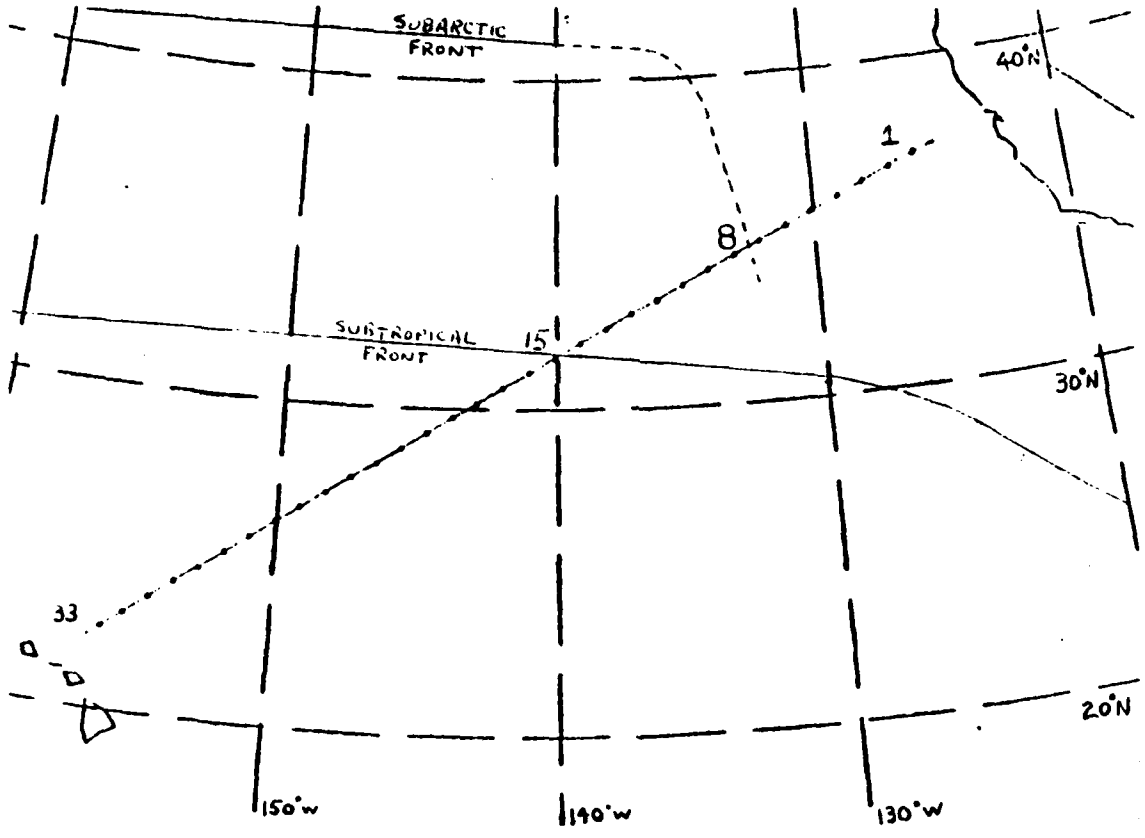

Fig. 1. Points along the San Francisco - Hawaii track for which calculations were made.

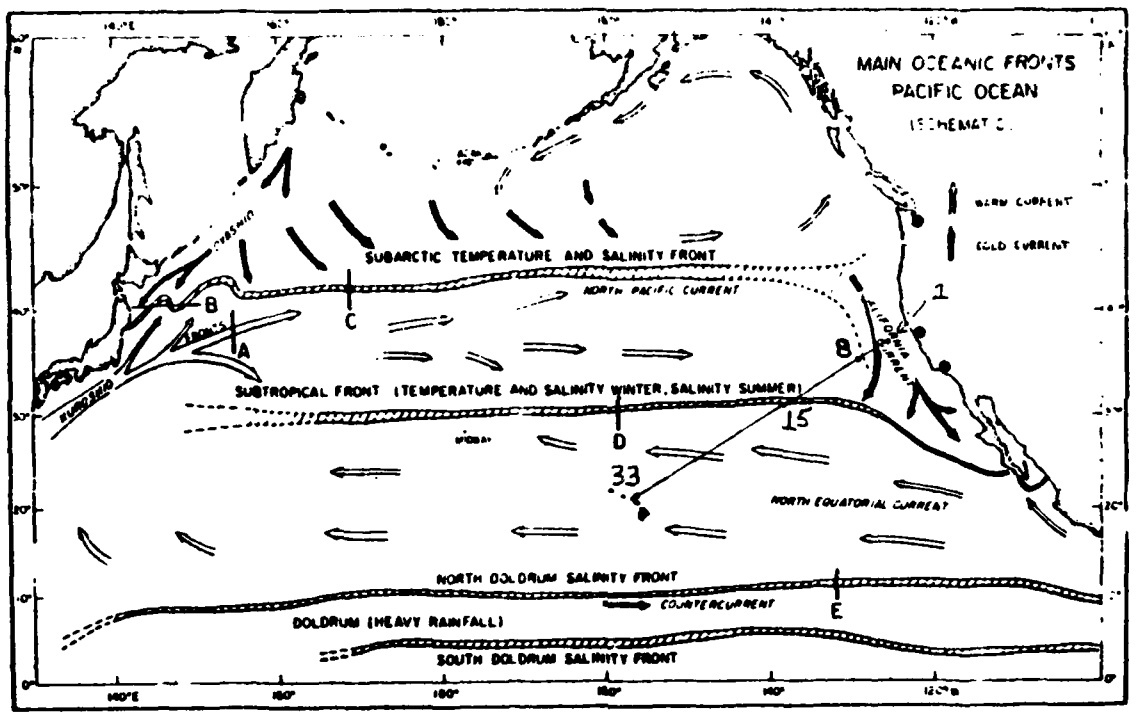

Figure II-1. Schematic map of main North Pacific fronts. Arrows indicate prevailing current directions. Letters refer to fronts: A, Kuroshio front; B, Oyashio front; C, subarctic front; D, subtropical front; E, doldrum front. (from Ref. II-1;

Fig. 2. Study track superposed on a physical oceanography map of the North Pacific ocean (reproduced from Saur (1980)).

one-dimensional model predictions over the various regions along the track will indicate the effect of these interactions and physical processes which have been assumed to be minimal.

II. DATA SOURCES AND PREPARATION

A. DATA SOURCES

The study was performed using data from two separate sources. Atmospheric forcing data were obtained from the Fleet Numerical Oceanography Center (FNOC) analysis and prediction fields on the Northern Hemisphere grid at 12-hour intervals. These data include total heat flux, solar heat flux, and the north-south and east-west wind components. In an independent project, Mr. P. Gallacher interpolated these data to hourly values on the 33-point grid. The techniques used to extract the hourly atmospheric forcing values from the FNOC fields are described in Gallacher (1979). Oceanic temperature profiles were provided by Dr. D. McLain of the Pacific Environmental Group, National Marine Fisheries Service. These profiles were obtained during a nine-year study in which merchant vessels, in transit between San Francisco and Hawaii, dropped expendable bathythermograph buoys approximately every four hours for ocean temperature data collection.

Atmospheric forcing data used in this study were a direct input to the Garwood mixed layer model at hourly intervals. Gridded oceanic temperature profiles were used to initialize the model runs and to verify the model output. No subsurface salinity profile information was available for this study, so a constant value of 35.0 parts per thousand was used.

B. VERTICAL INTERPOLATION

The oceanic profiles were first vertically interpolated to a standard grid of 5 M spacing, and values to 200 M were stored. An important part of this vertical interpolation scheme was the determination of the mixed layer depth. There is no concensus method for determining the mixed layer depth when analyzing a temperature profile. It appears that various definitions have been applied in different locations, depending upon the requirements (operational or research) and profile resolution. In this study, the mixed layer depth has been defined to be that depth at which the temperature profile changes from a relatively isothermal one to that with a decrease in temperature exceeding 0.10°C in 5 M.

A feature which appeared in many of the temperature profiles was a slight increase in temperature with depth in the upper 50 M of the profiles, and this was followed by the expected large negative gradient below. Because the model required that all input profiles be stable, and since no salinity information was available to support this unstable thermal condition, the upper-level temperature structure was adjusted to be isothermal above the mixed layer depth. This was accomplished by obtaining an average temperature above the mixed layer depth, and modifying the profile such that the temperature was isothermal down to the point where this average temperature intercepted the original profile.

C. OBJECTIVE ANALYSIS

Vertically gridded buoy data required adjustment to a horizontal grid with regular space and time intervals to serve as initial and

verifying data for the model predictions. Several forms of horizontal adjustment of this ocean temperature profile data set have been employed. Saur (1980) applied a least-squares fit for the eight closest buoys to any gridpoint. Dorman and Saur (1978) calculated anomalies of temperature from the mean seasonal cycle and used time-space correlations of these anomalies to analyze objectively onto a standard grid. In this study, the profiles were horizontally interpolated in time and space to the selected gridpoints using a modified Cressman (1959) technique of decreasing range weighted corrections. Decreasing radius time increments from two weeks to one-half week were used. Elliptical space increments, with the major axis oriented along the track, were used because the actual ship tracks deviated from the great circle route. The semi-major axis decreased from 1.75 to 1.1 times the grid spacing (Fig. 3). A total of 4 scans were employed for both time and space. The range of the weighted scans was selected to be consistent with the time and space scales used in the study, and to provide realistic output profiles with a reasonable time and space relationship between adjacent points.

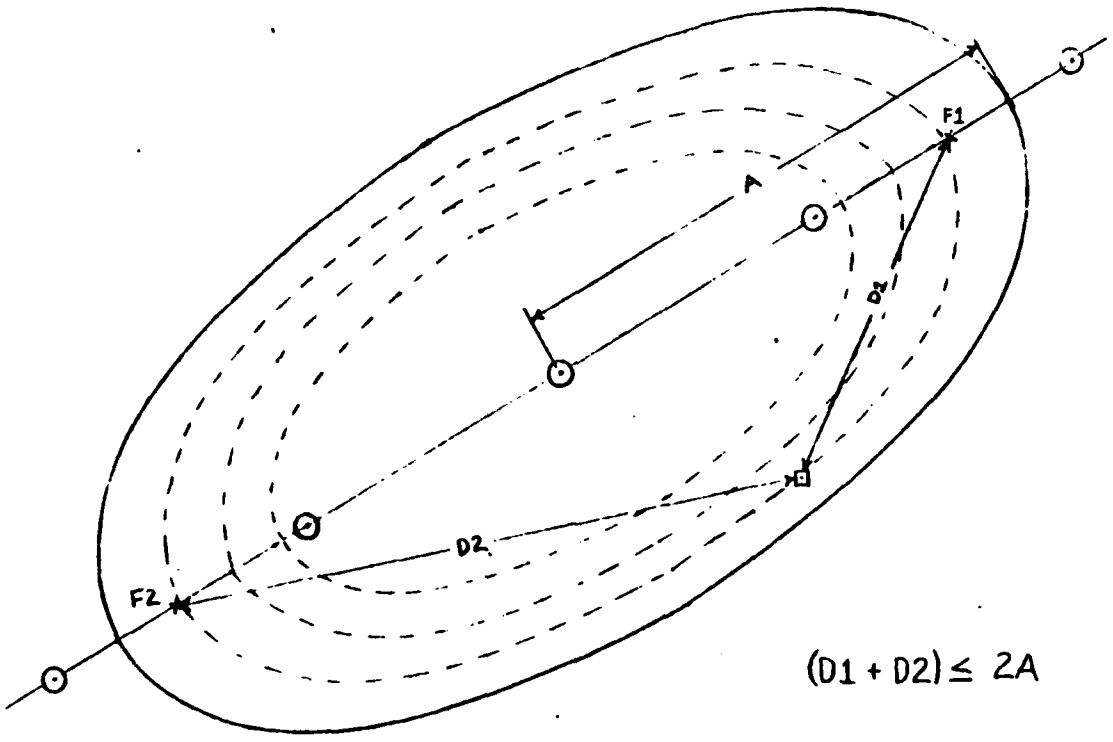

Fig. 3. Modified Cressman objective analysis scheme using ellipses with the semi-major axes oriented along the study track. The maximum distance allowed in a scan is two times the semi-major axis distance.

III. HEAT BUDGET

A. BASIS

A simple heat budget calculation was made prior to using the data in the model. Under the assumption that the vertical processes dominate the horizontal, and for the space and time scales in this study, the local change in heat content in the ocean over a given period should be balanced by the total vertical flux of heat at the air-sea interface. This has been shown, by Gill and Niiler (1973), to be true for time scale on the order of a season. They also showed that the larger the region, the smaller the effect of horizontal advection. This theory has been tested and shown to be generally valid for the eastern North Pacific ocean in a study by Schnoor (1975). Following Schnoor, the conservation of heat equation of Wyrtki and Haberland (1968) has been reduced to a simplified form:

$$Dh/Dt = Q + (\text{Sum of subsurface processes}) \qquad (1)$$

The term on the left hand side denotes the local rate of change of total heat storage, where H is determined for the upper 200 M of the ocean by:

$$H = \int_{-200}^{0} \rho c T \, dz \qquad (2)$$

For the purposes of this study, the most recent value of H is subtracted from the prior value to determine the rate of change of H. The first term on the right hand side denotes the net heat flux at the air-sea interface during the same time period, while the second term on the right hand side includes horizontal advection and diffusion. If atmospheric

and oceanic data are assumed to be perfectly measured and analyzed, we can determine the magnitude of these processes in a local area by calculating the difference between the observed change in oceanic heat content and the analyzed surface flux of heat for that area.

B. METHOD

The heat content in the upper ocean layers was calculated using a trapezoidal integration scheme over the upper 200 M, and then subtracting the value at 200 M to normalize the results. The change in heat content was considered over 2-month intervals and applied at the midpoint of the interval. The observed changes in oceanic heat content converted to average hourly values are shown in Figure 4. The sign convention is consistent with that for surface heat flux, i.e., a negative value indicates a gain in heat content in the ocean, which corresponds to a net downward heat flux (also negative). Figure 5 is a similar display for the hourly average values of accumulated total heat flux at the air-sea interface, which is derived from the FNOC fields. The field for the atmospheric forcing has a much more uniform horizontal variation than does the change in heat content, since the heat flux has been interpolated from a much larger grid than the grid used in this study. Several large amplitude variations along the track in the heat content field during late summer and early fall are noted. The change in oceanic heat content field also includes a much larger spatial and temporal domain of negative values (corresponding to downward heat flux), especially during the summer months over the southern half of the track. The surface heat flux values indicate a bias toward excessive upward heat flux. This is most

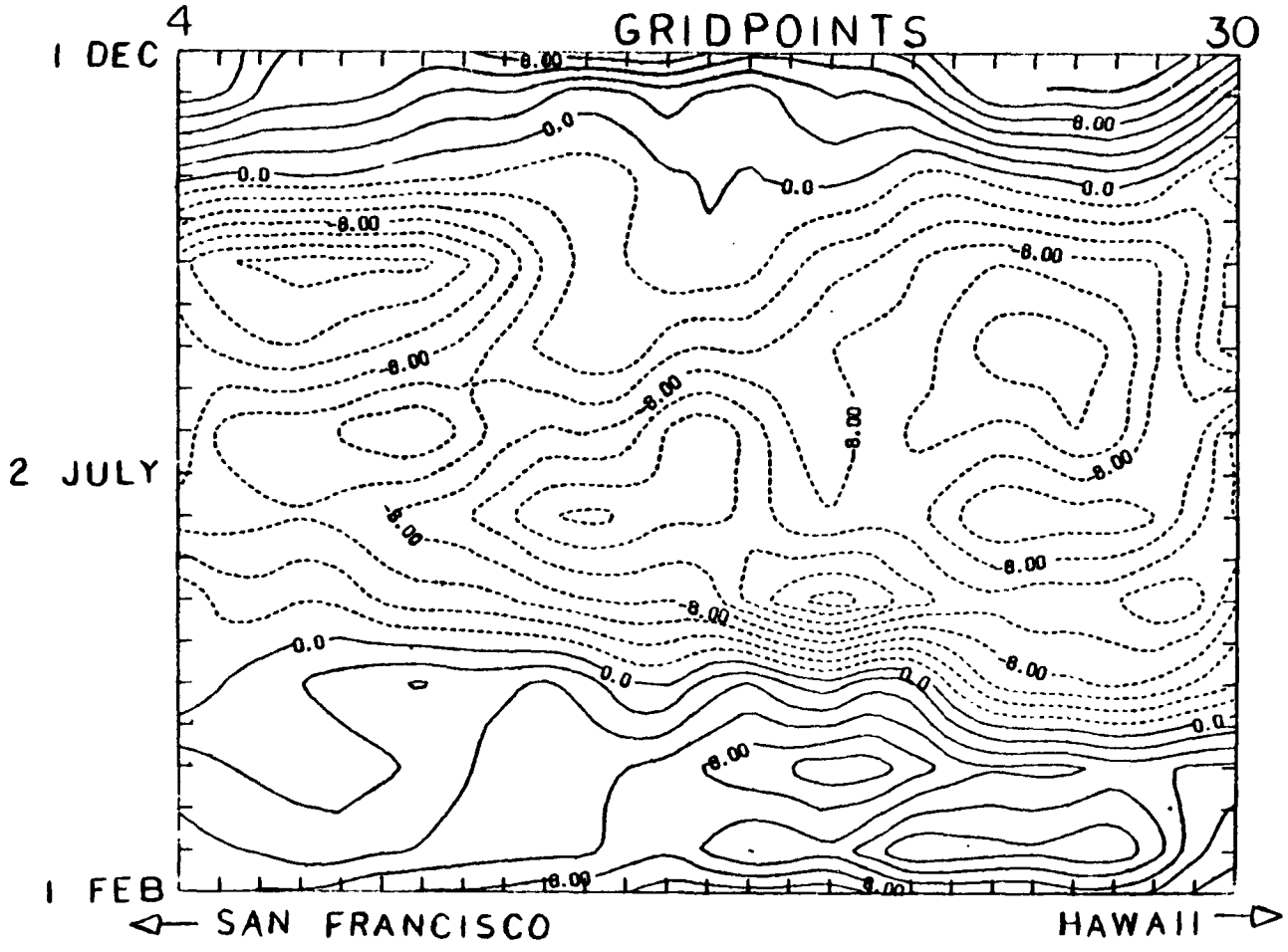

Fig. 4. Observed change in oceanic heat content (ly/hr) for gridpoints 4-30, from 1 February to 1 December 1978. Values are hourly averages obtained from two-month differences, and applied at the midpoint of the interval. A negative value indicates a gain in oceanic heat content.

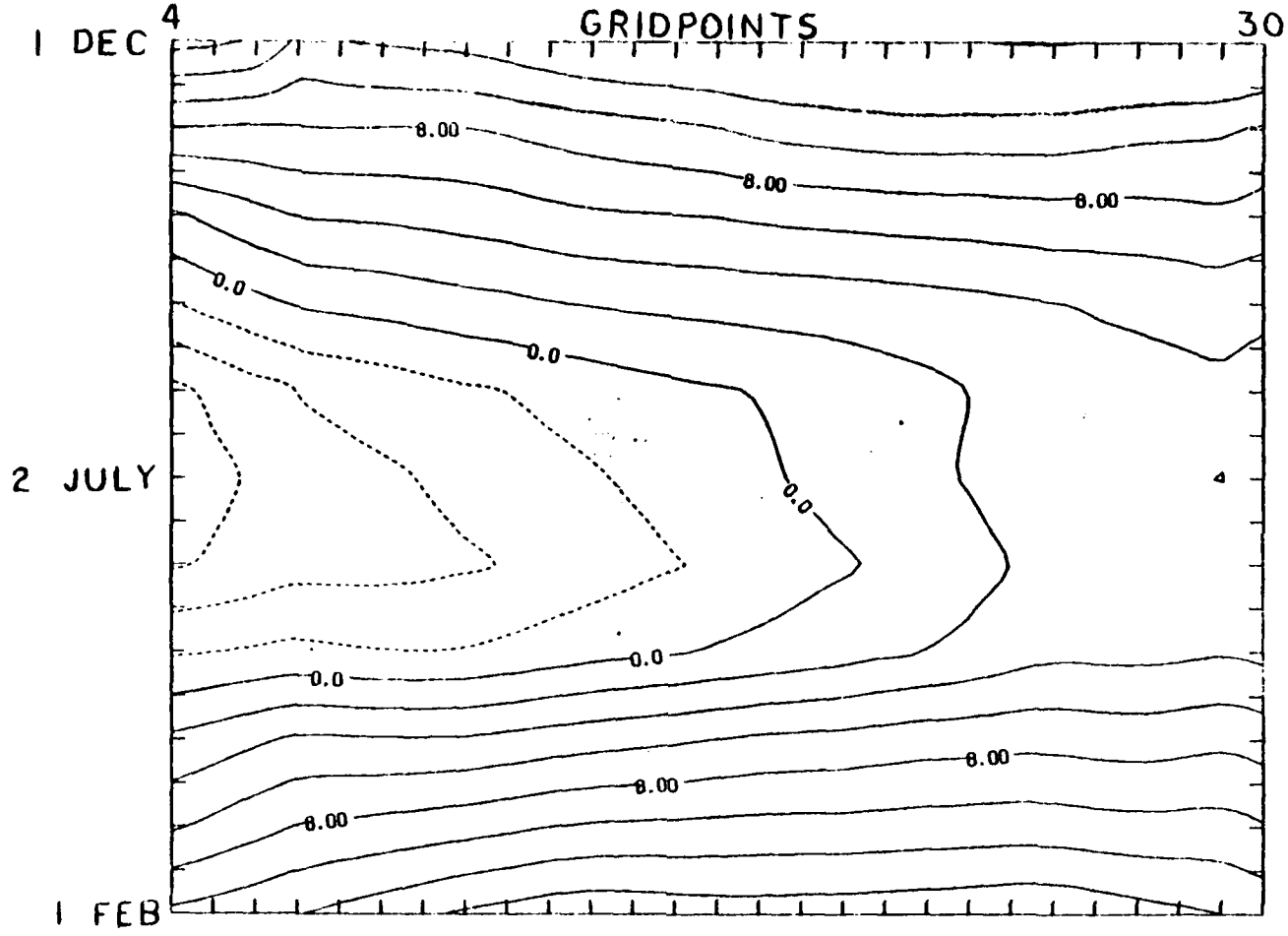

Fig. 5. Cumulative surface heat flux (ly/hr) for gridpoints 4-30, from 1 February to 1 December, computed from FNOC atmospheric prediction model. Values are hourly averages obtained from two-month differences, and applied at the mid-point of the interval. Negative values indicate net downward heat flux.

evident in the summer over the southern part of the grid, where the average monthly values indicate net cooling rather than heating of the ocean. The bias appeared to increase in magnitude as the boundary of the Northern Hemisphere grid was approached. A similar problem was found by Elsberry, Gallacher and Garwood (1979). Budd (1980) found that mixed layer depth predictions were unrealistic and determination of spring transition dates was difficult in this latitude belt until a correction to the cumulative surface heat fluxes was made. Budd showed that it was feasible to reduce the disagreement between observed and predicted values of mixed layer depth by correcting the total heat flux field.

In the general case, the imbalance between these two fields can indicate error in either term, or a deviation from local heat balance. It is clear that the major error is in the heat flux field. However, the possibility of errors in the heat content field, or of a deviation from a local heat balance still exists.

To apply a uniform long-term correction to the total surface heat flux field, it was necessary to eliminate features in the change in heat content field which are random errors or are transient features superposed on the long-term field. The smoothing process involved several steps. A quasi-periodic fluctuation along the track was eliminated by using a 6-point running filter. Attempts using 5-,7-,8- and 9-point filters produced much less uniform results. A comparison of January 1978 results with 6-point and 9-point filters is given in Figure 6. This figure indicates that the total surface heat flux values are greater than the observed change in heat content values over

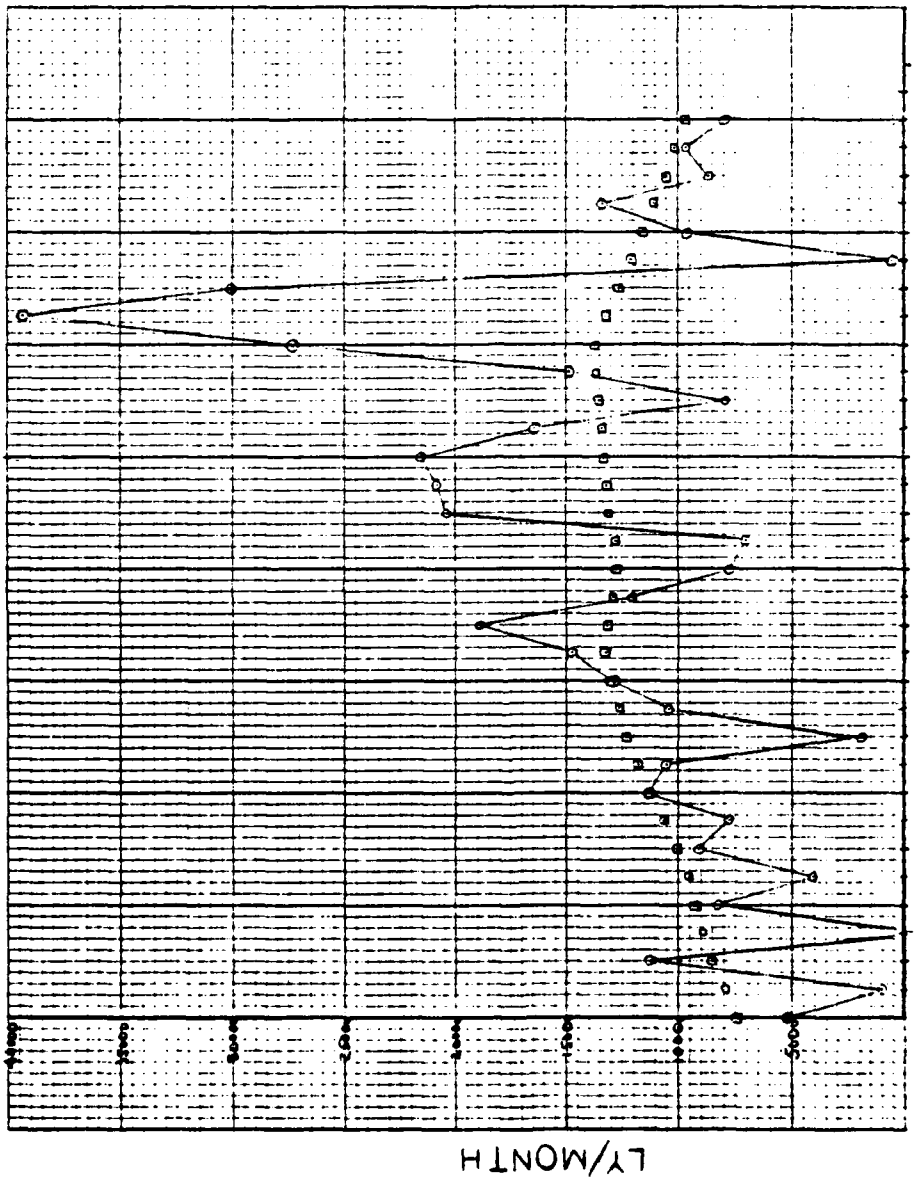

Fig. 6a. Unsmoothed monthly heat content values (solid line) and accumulated surface heat flux (LJ) (ly/month) for January, 1978.

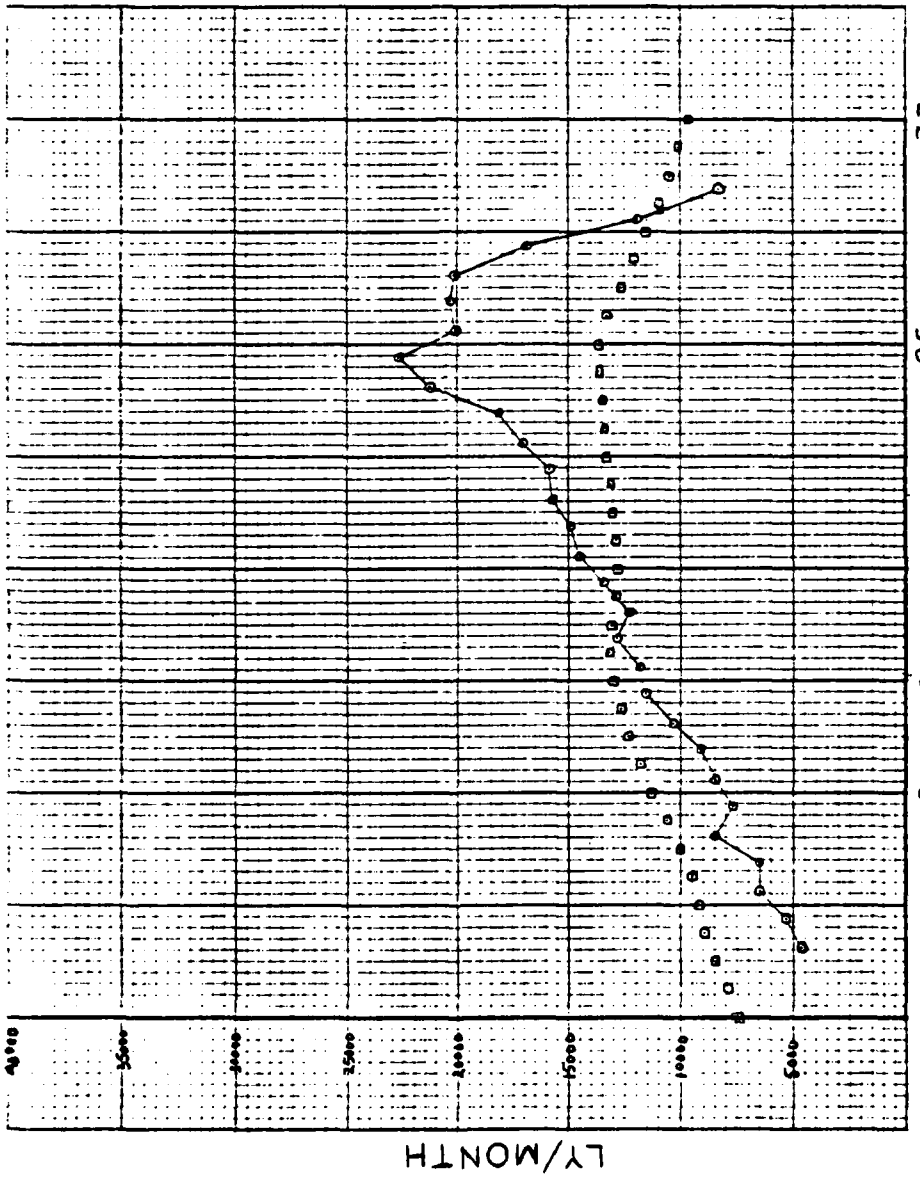

Fig. 6b. Similar to Fig. 6a, except for 6-point smoothed values.

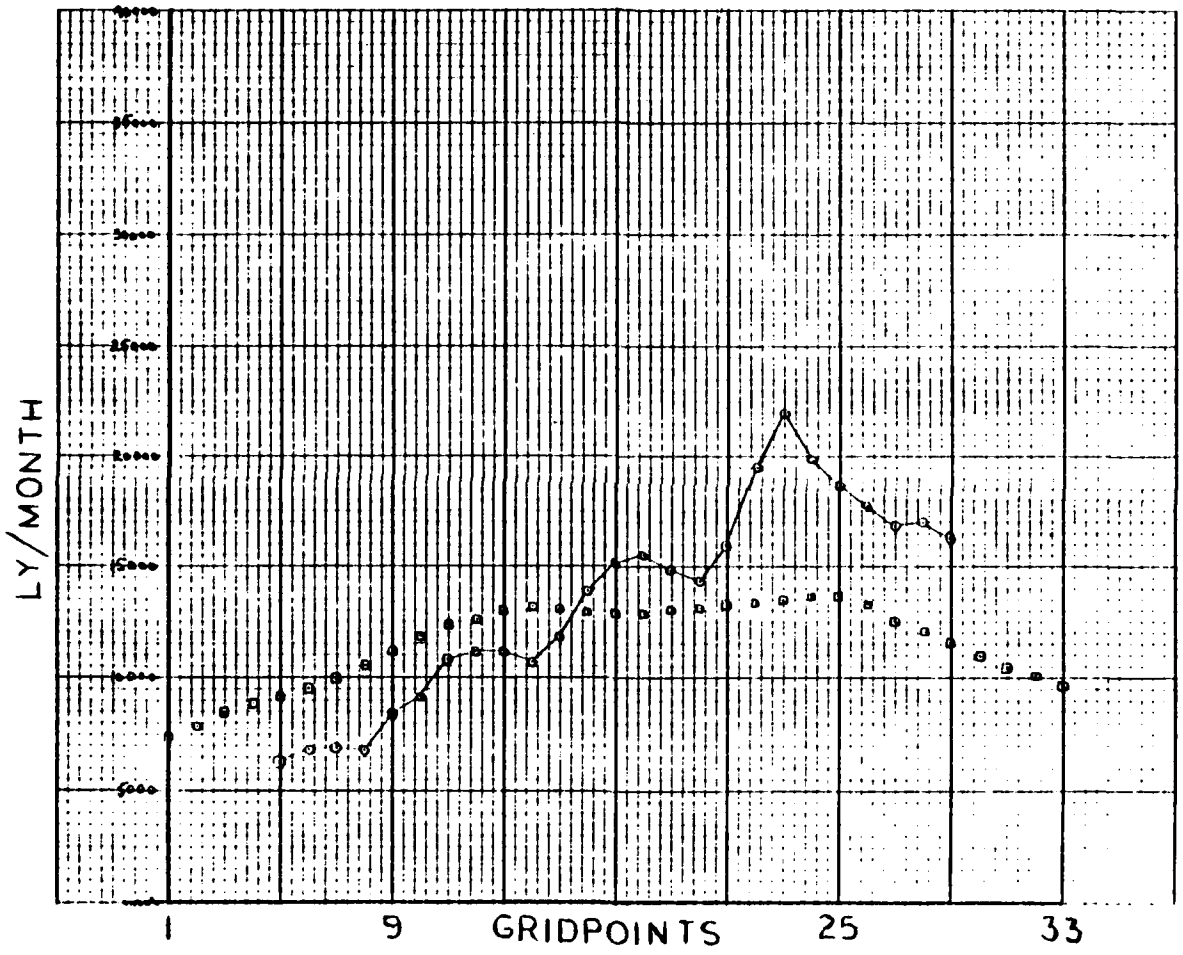

Fig. 6c. Similar to Fig. 6a, except for 9-point smoothed values.

the northern part of the track, while the heat fluxes are much lower over the southern portion of the track. This bias appeared in all filtered and unfiltered results and does not appear to be a product of smoothing. Short term fluctuations were eliminated by taking the difference in heat content over two months. Attempts using differencing over shorter time intervals produced much less uniform results. Three-month differencing also did not improve results, as indicated in Figure 7. It was felt that the selection of even greater time intervals would tend to produce smoother results. However, longer time intervals were considered to be less representative of the time scales of the processes involved in the local heat balance than the two-month differencing.

After selection of a two-month difference and application of a 6-point filter, the smoothed field still contained a number of features which were either transient phenomena or which represented actual permanent deviations in the local heat content from a uniform field. The difference between the total surface heat flux and observed oceanic heat content fields is illustrated in Figure 8. The almost universal range of positive values in Figure 8a indicates that excessive upward heat flux exists throughout the region, and over the entire year. Figure 8b clearly shows, for the southern part of the track, that total surface heat flux obtained from FNOC analysis remains positive throughout the year, with a minimum near zero in the summer. The observed change in oceanic heat content for the same area indicates the expected trend for large downward heat flux during the summer. A comparison was made of the 1978 change in heat content values with

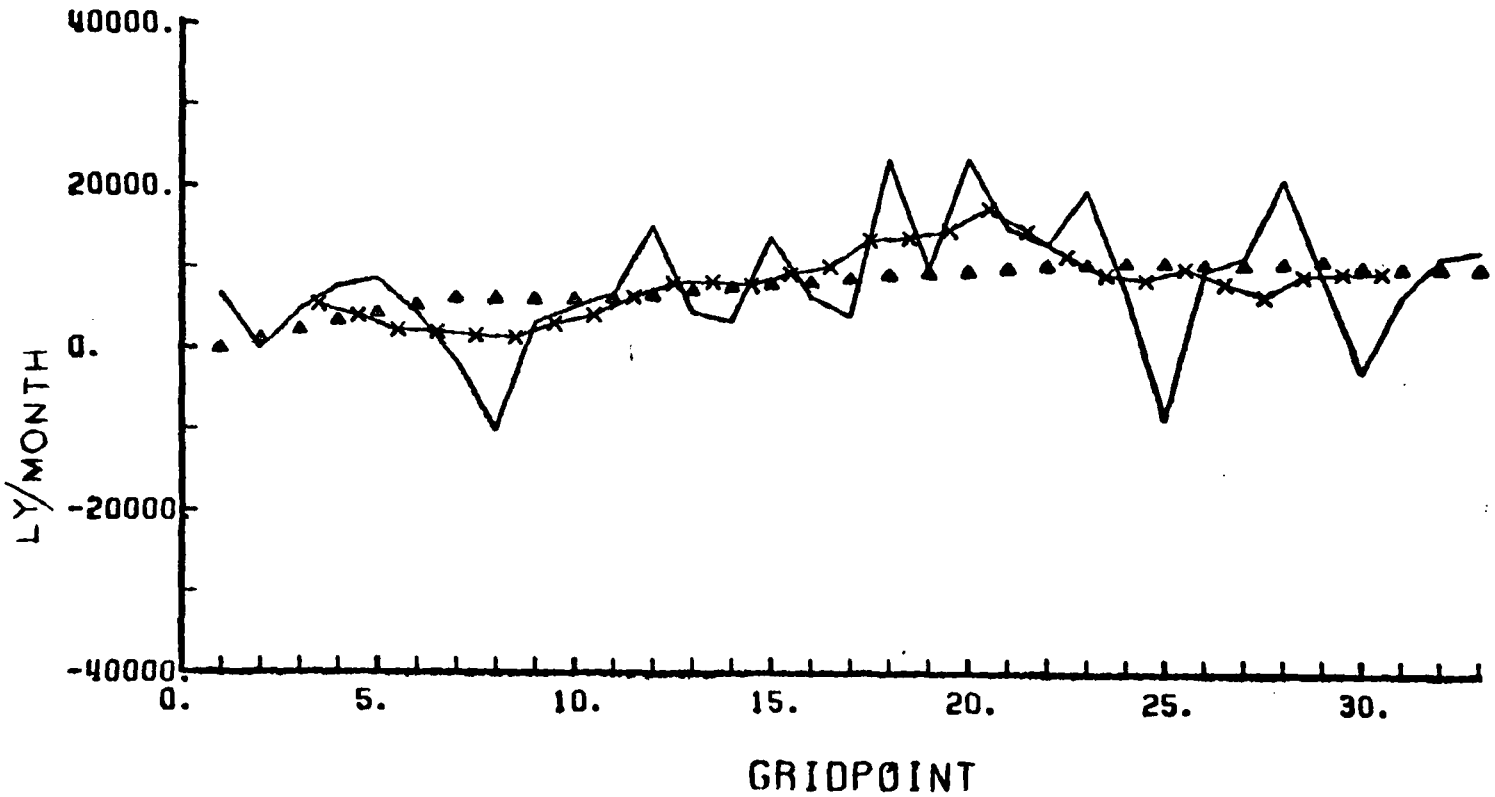

Fig. 7a. Accumulated surface heat flux (△), unsmoothed heat content (solid line) and 6-point smoothed heat content values (x) (ly/month) for March-April using two-month differencing.

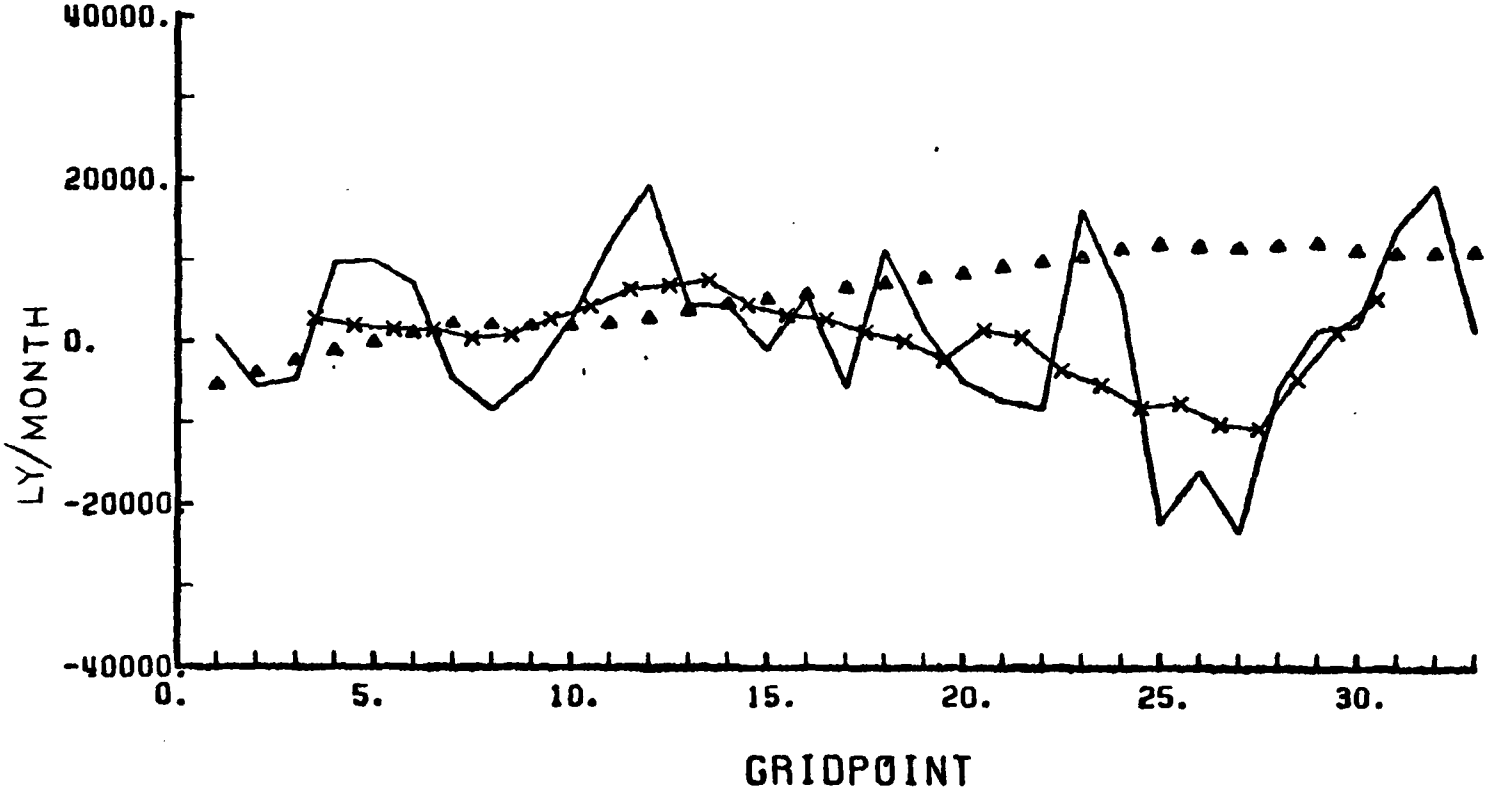

Fig. 7b. Similar to Fig. 7a, except for March-May 1978 using three-month differencing.

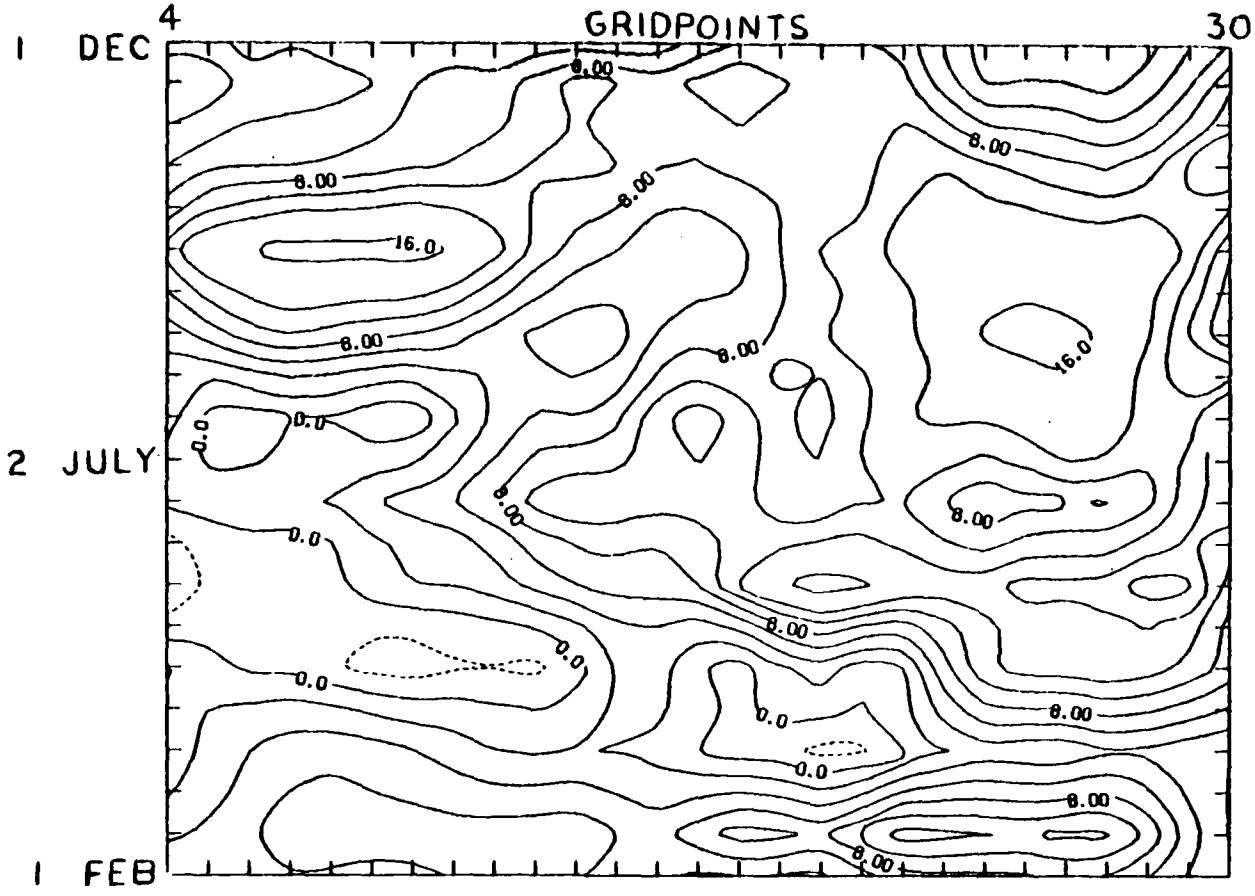

Fig. 8a. Difference between accumulated surface heat flux and observed change in oceanic heat content (ly/hr), with hourly average values, as before. Solid lines indicate that upward heat flux exceeds the net change in heat content.

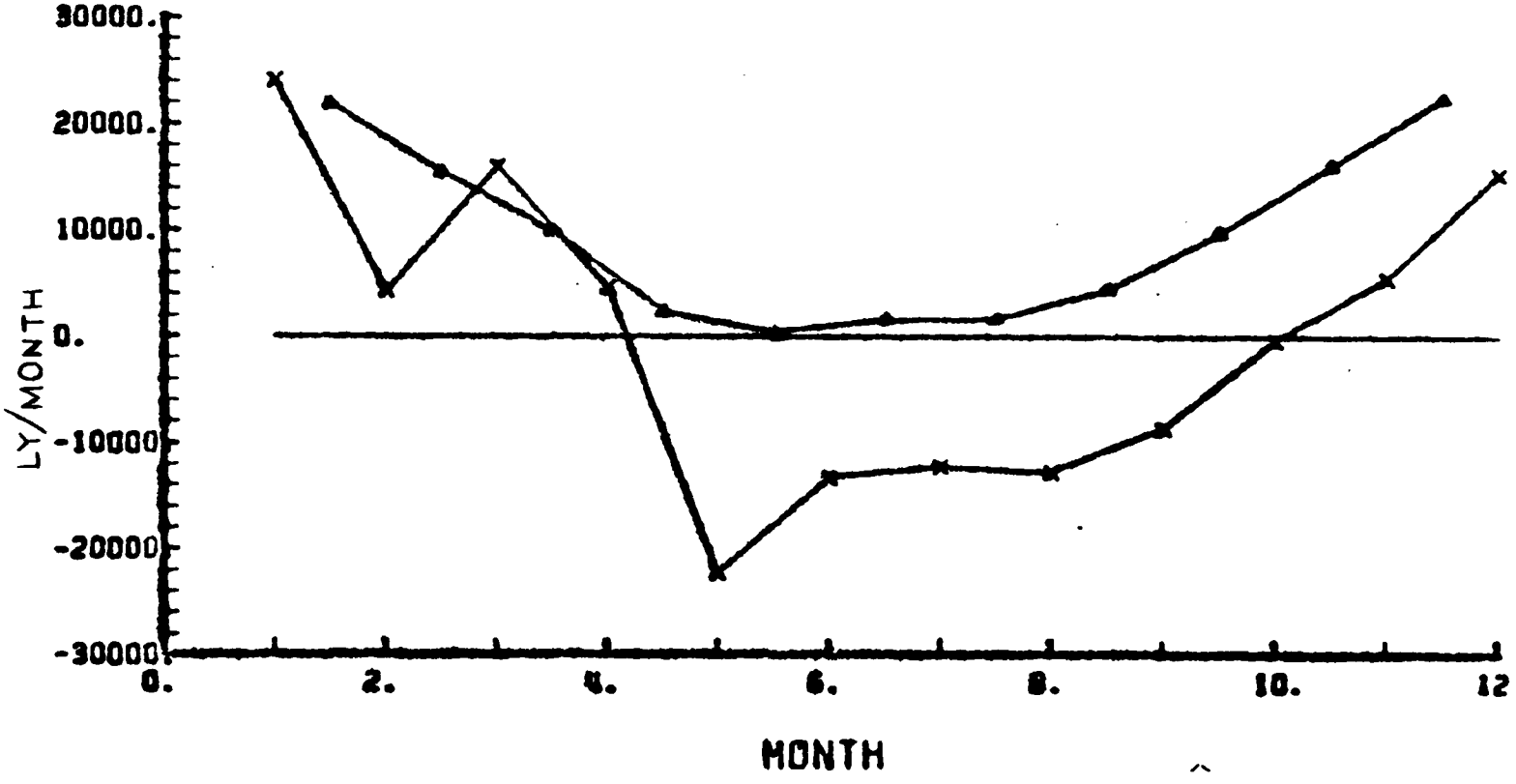

Fig. 8b. Accumulated surface heat flux (△) and observed change in oceanic heat content (X) (ly/month) for gridpoint 21.

similar values for 1976. The difference between the 1976 values and the 1978 values of change in heat content is depicted in Figure 9a. It is clear that the major deviations in the 1978 data are transient in nature, since the 1976 field shows a number of deviations that are opposite in sign for the same time periods (Fig. 9b). Thus, the 1978 field was further hand-smoothed to obtain a long-term profile, which can be approximated by averaging the 1976 and 1978 fields. The smoothed 1978 change in heat content field was then compared to the total heat flux field. A bias toward excessive upward heat flux throughout the year over most of the grid was observed. A monthly correction to be applied to the total heat flux field was calculated from the difference from the change in heat content field. This correction field, converted to hourly values, is shown in Figure 10. Large values must be subtracted to reduce the upward heat flux in the total surface heat flux field, over most of the area, thoughout the year. Correction values tend to increase toward the south, as in a similar correction field derived by Budd (1980). The smoothed change in heat content field and corrected total heat flux fields are shown in Figures 11 and 12, respectively. The two fields show a similar spatial and temporal arrangement of smooth areas and large amplitude features, indicating a near local heat balance on a two month time scale. However, predictions using the corrected total surface heat flux field will generally be on shorter time scales.

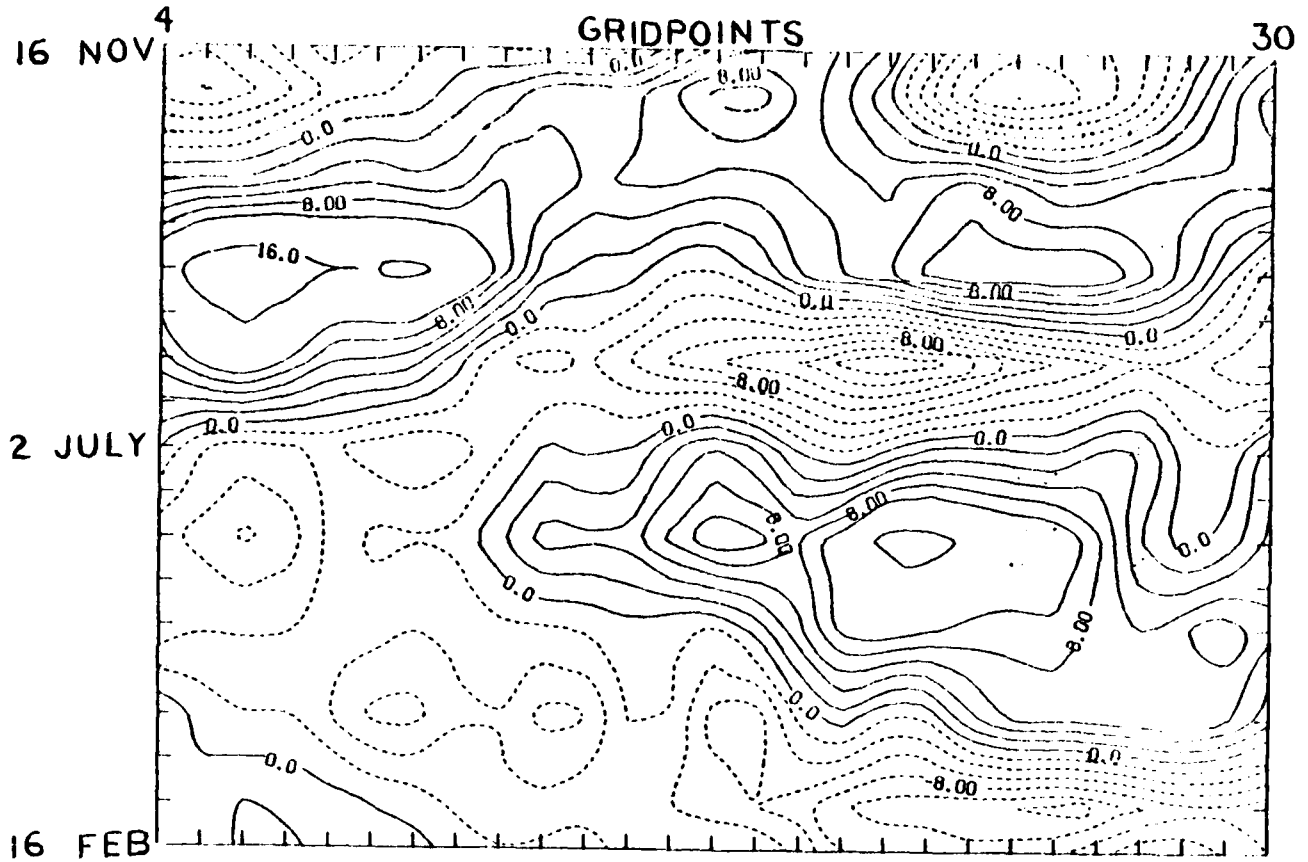

Fig. 9a. Difference between 1976 and 1978 observed change in oceanic heat content (ly/hr), with hourly values as before.

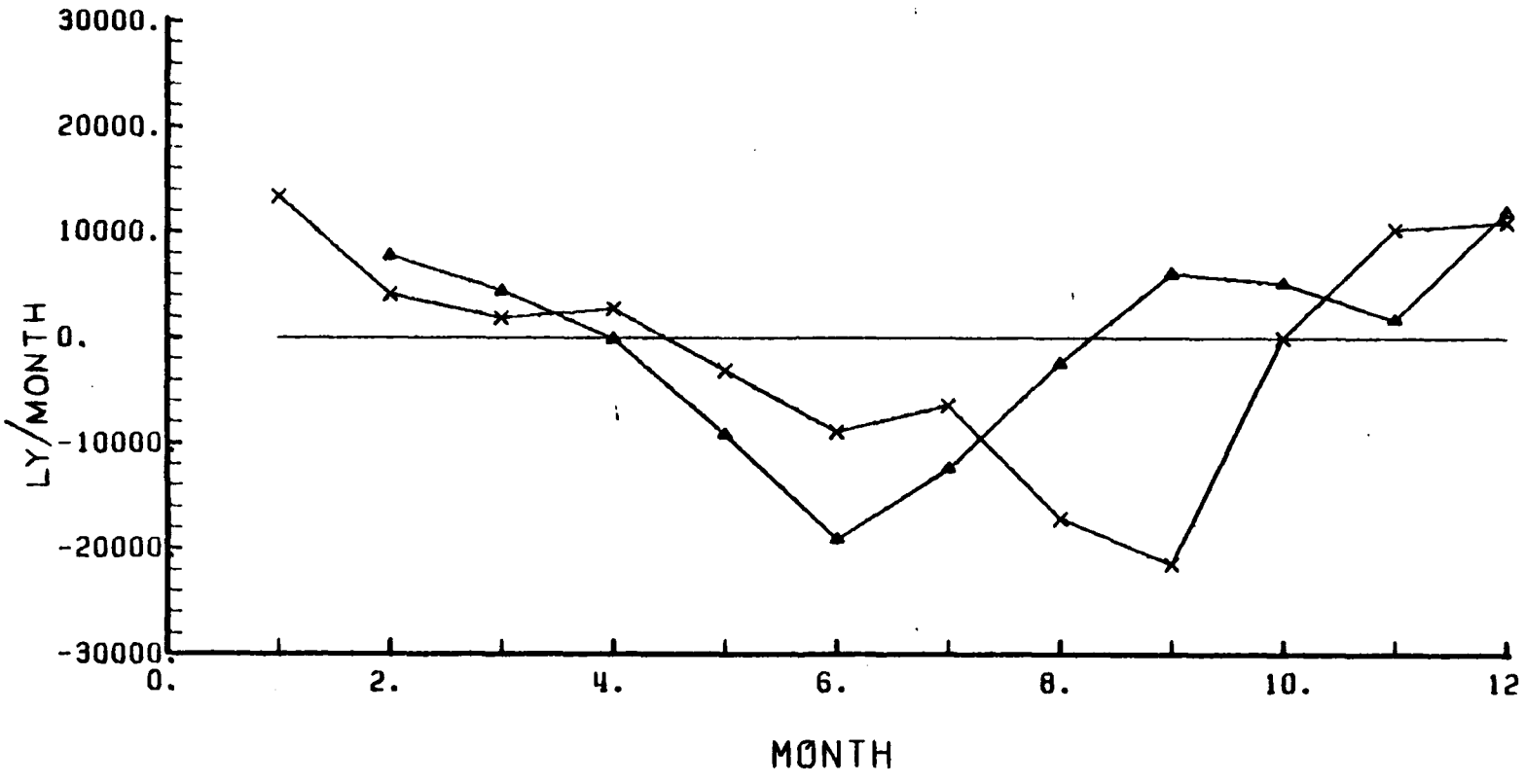

Fig. 9b. Observed change in heat content for 1976 (△) and for 1978 (x) (ly/month) for gridpoint 7.

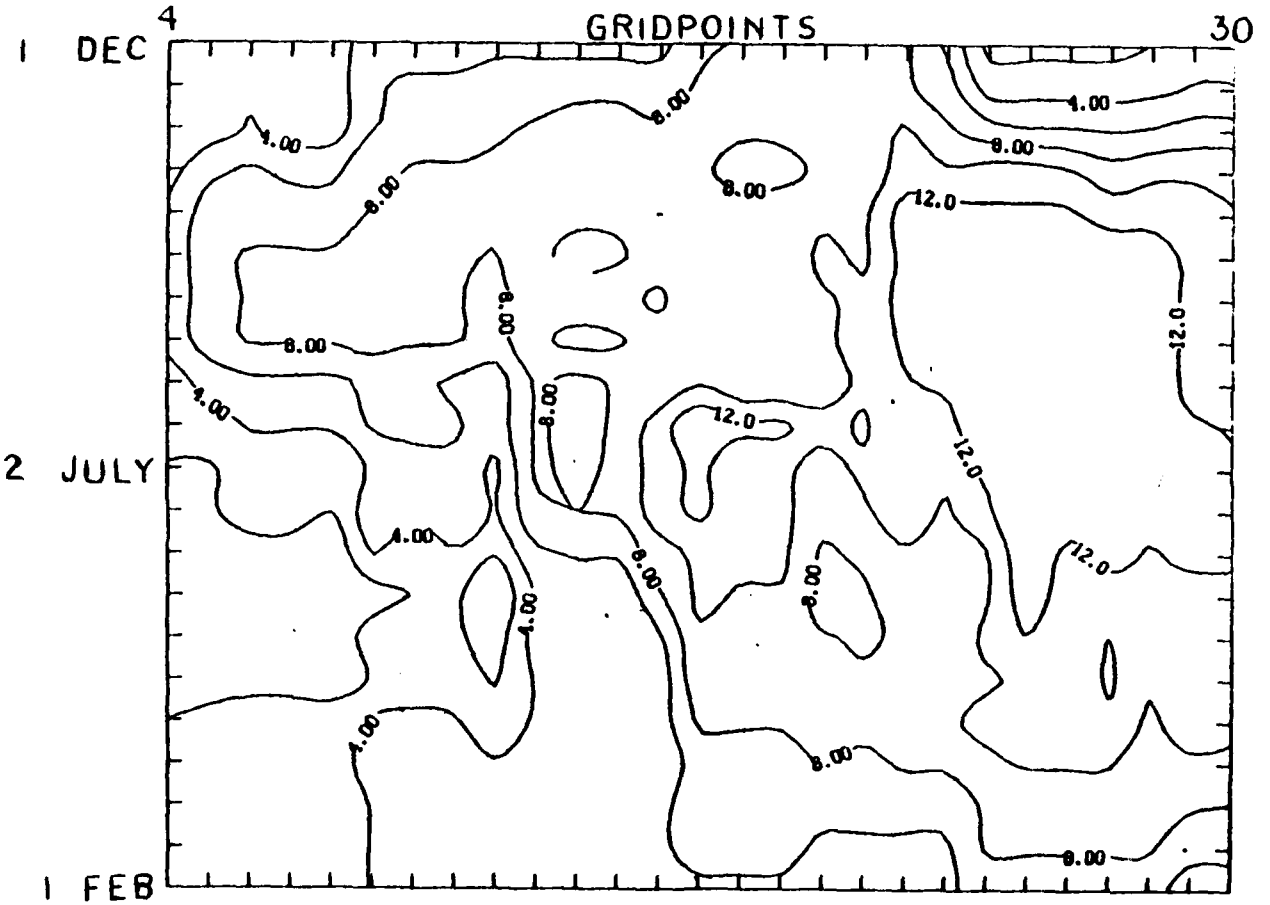

Fig. 10. Cumulative surface heat flux correction field. Solid lines represent values to be subtracted from the FNOC heat flux values (ly/hr).

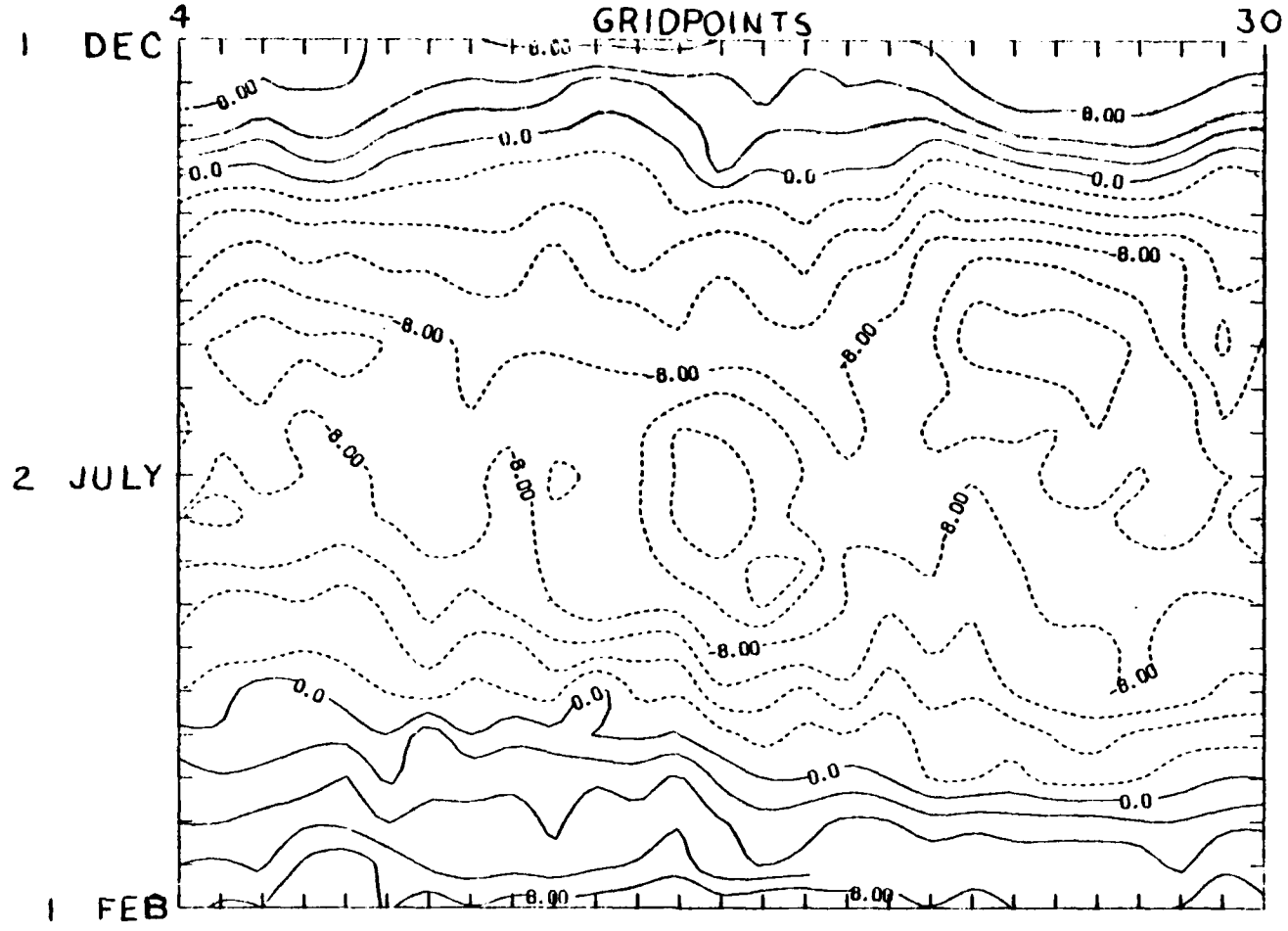

Fig. 11. Smoothed version of Fig. 4.

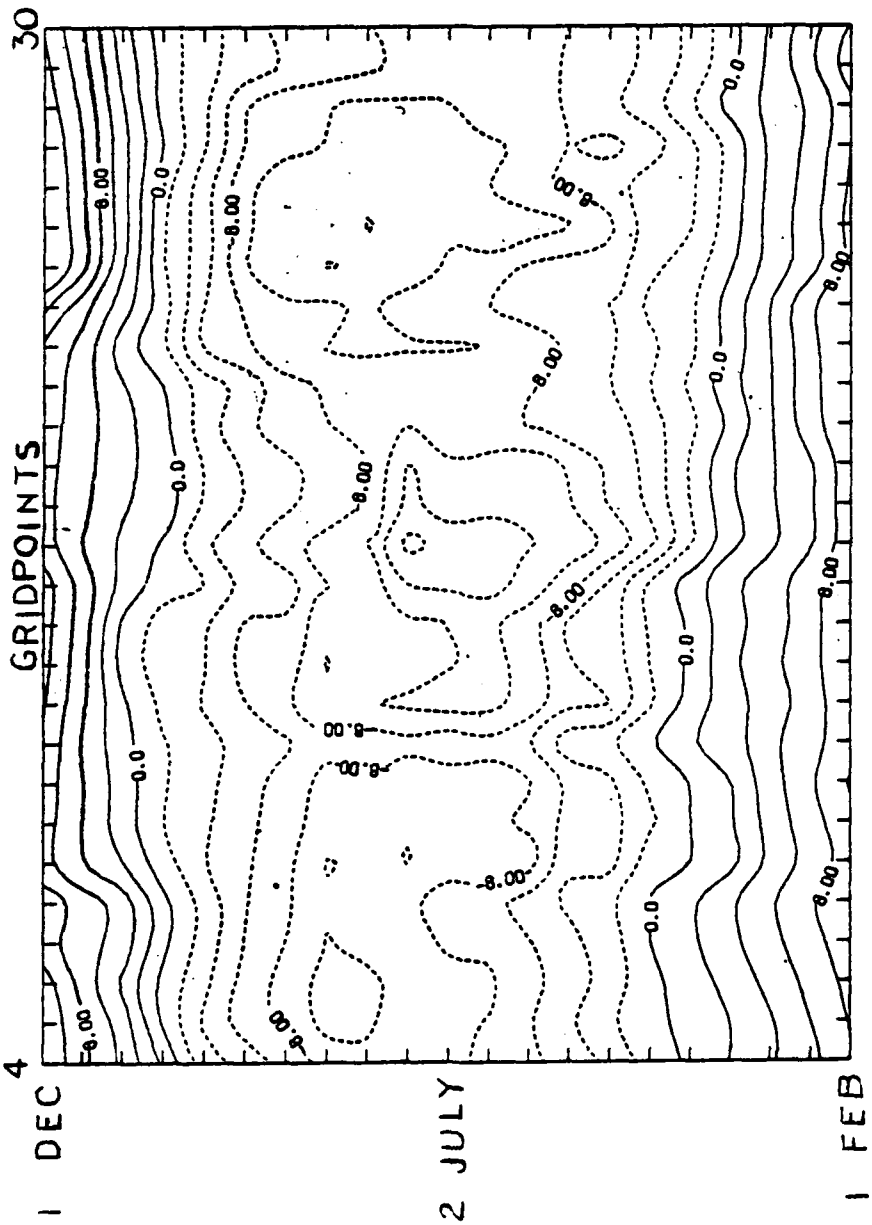

Fig. 12. Corrected version of Fig. 5.

IV. PROCEDURES

A. TYPES OF RUNS

The study consisted of two major types of computer model runs. A series of long-term runs was made by initializing the model with the 1 February temperature profiles, and verifying the model at each 15-day interval until 16 December. The other series of runs consisted of initializing the model at each 15-day interval and verifying at each subsequent time level for 60 days. Model error results for 15-day predictions from each of the short term runs were combined. A similar procedure was followed for the 30-,45- and 60-day results. This allowed for an overall comparison of model performance throughout the year at approximately 2-,4-,6- and 8-week intervals, respectively.

B. TYPES OF ANALYSIS

Input parameters for all model runs included the atmospheric forcing functions at hourly intervals. Output parameters included a temperature profile with values at every 5 M down to 200 M, and the associated model-determined mixed layer depth. Since temperature changes below the thermocline are very slight, the values of interest in this study were the mixed layer depth and the mixed layer temperature. Because model temperatures above the base of the mixed layer are isothermal, the sea surface temperature was used in the verifications.

Three types of model predictions were verified. Model profiles at the exact time of the verification profiles were designated as "model"

runs. Model profiles obtained by averaging all of the hourly model profiles from 84 hours prior to verification time to 84 hours after that time were designated as "average model" runs. Some model comparisons were also made using profiles obtained by averaging only the profiles with the maximum mixed layer depth for each 24-hour period, in the same 168 hour period used for the average model profiles. These were designated as "daily max' runs. These model-predicted profiles were compared to "predictions" of climatological profiles and persistence profiles in all runs. The climatological profiles were derived from the vertical sections of semimonthly mean temperatures for the period June 1966 to December 1974 described in Saur, Eber, McLain and Dorman (1979).

Comparisons were made between mixed layer depths obtained from the various prediction methods and the objectively analyzed mixed layer depths for the long-term runs. A similar comparison was made for the sea-surface temperature. These comparisons were useful for determining the accuracy of prediction of major events such as the spring transition, the stable summer period and the fall deepening period. In turn, general trends in model bias could be easily identified by these comparisons.

The comparisons made for the 60-day runs consist of examining the bias and root-mean-square errors for the various predictors, and the trends in these errors. Values at gridpoints with common errors were combined to obtain area comparisons. Seasonal comparisons were also performed over two month time periods. These comparisons made possible the determination of areas or times when large model errors were related to external factors not included in the model.

V. RESULTS AND ANALYSIS

A. LONG-TERM RESULTS

The progression of the mixed layer depth for gridpoints 13 and 4 is shown in Figures 13 and 14. These gridpoints represent areas where the model performance differed greatly. Gridpoint 13 was representative of an area from gridpoints 8-19 in which the model did relatively poorly. Gridpoint 4 was representative of the area from gridpoints 1-7 in which the model performed relatively well. Model performance for the area of gridpoints 1-7 was better for mixed layer depth prediction than for mixed layer temperature prediction. Each figure shows a comparison between average model results, actual profiles, and climatology. Figures 15 and 16 show the same comparisons for sea-surface temperature for gridpoints 13 and 4, respectively. A long-term model bias toward overly-shallow mixed layer depths at gridpoint 13 can clearly be seen in Figure 13. However, Figure 14, for gridpoint 4 appears to be very accurate throughout the year, with a slight bias toward shallow mixed layer depth. Mixed layer depth prediction for the southern part of the track also showed excellent agreement between average model predictions and analyzed profiles. A comparison of climatology with analyzed profiles at the two gridpoints indicates that gridpoint 13 experienced an early spring transition, and mixed layer depths slightly deeper than average during summer and fall, while gridpoint 4 experienced spring transition at the usual time of year, and mixed layer depths close to climatology throughout the year. In general, spring transition occurred earlier that normal over most of the track.

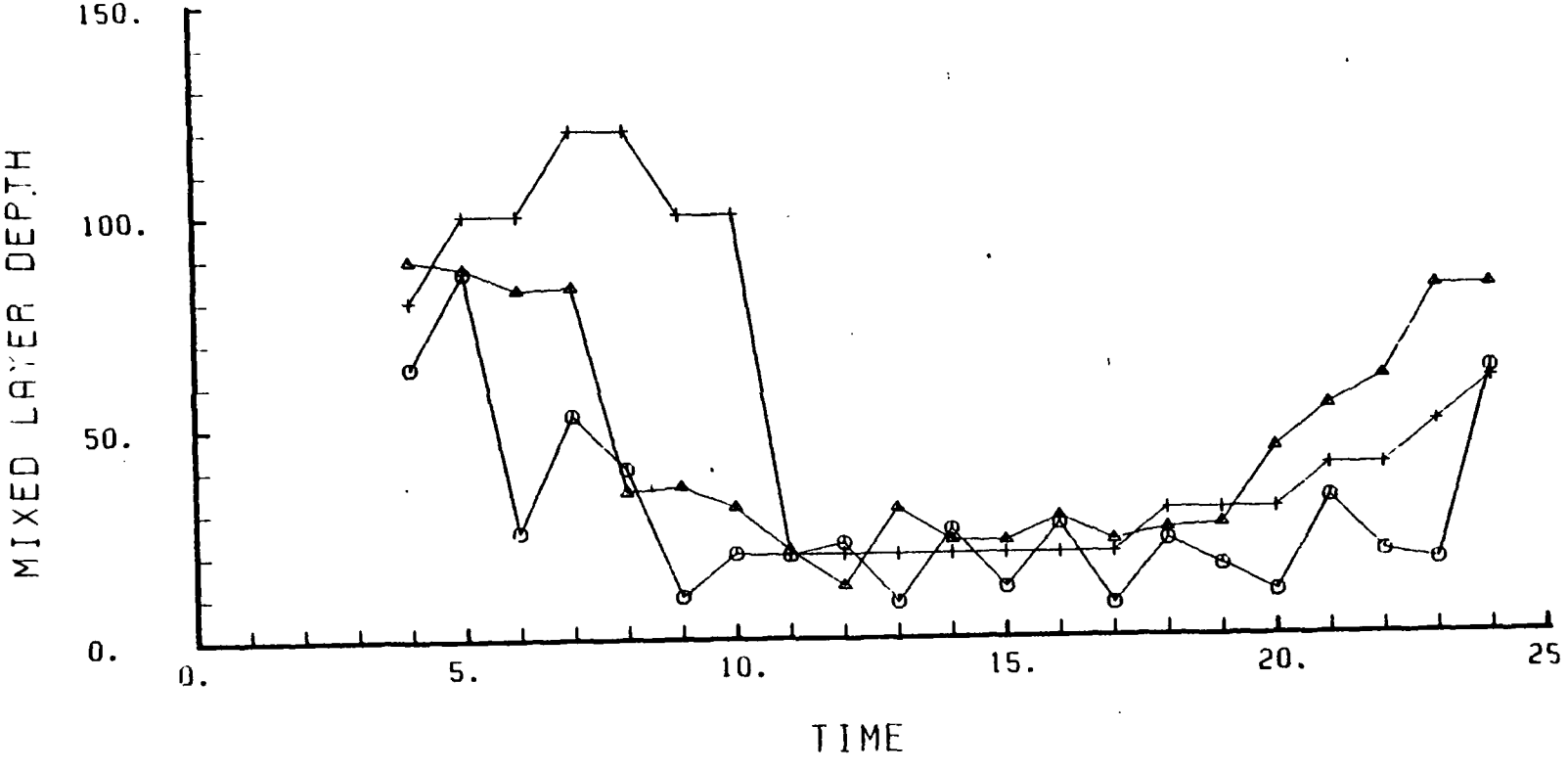

Fig. 13. Mixed Layer Depths (M) plotted at 15-day intervals (time 1 = 1 January 1978) for a forecast initialized on 1 February 1978 and ended on 16 December 1978 at gridpoint 13, for: Model profile = O , Climatology profile = + , Actual profile = △ .

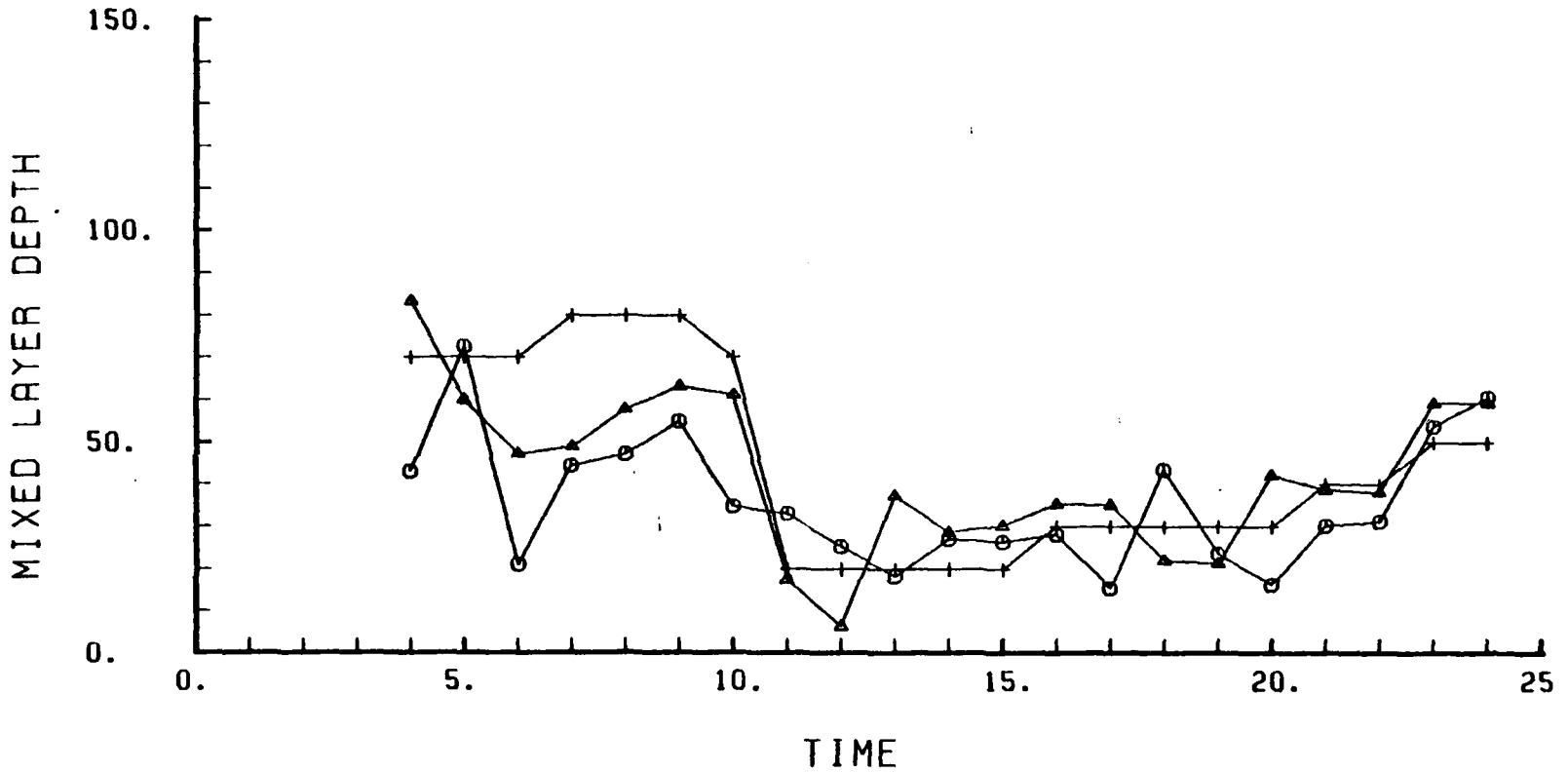

Fig. 14. Similar to Fig. 13, except at gridpoint 4.

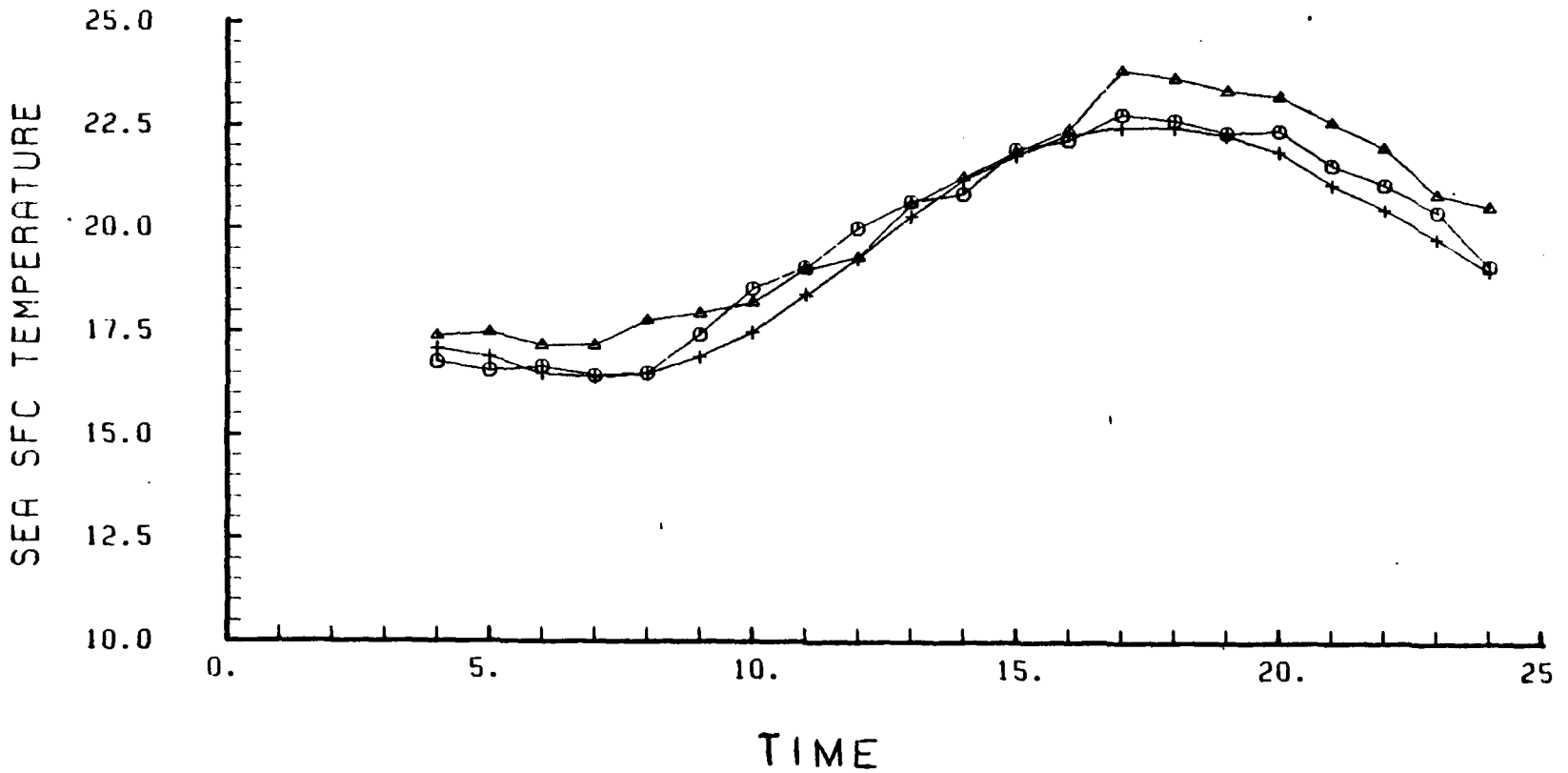

Fig. 15. Similar to Fig. 14, except for sea surface temperature (°C).

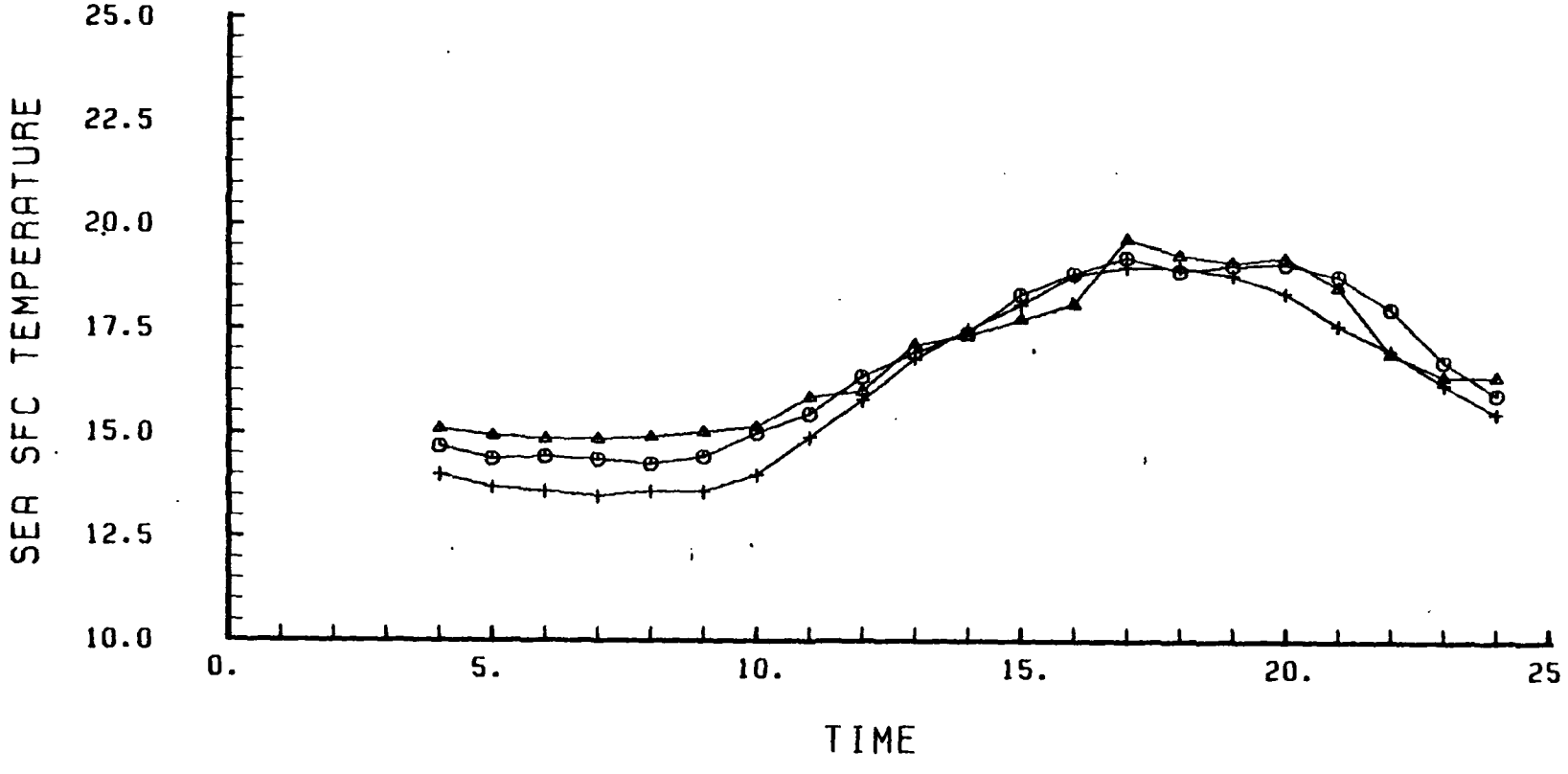

Fig. 16. Similar to Fig. 15, except at gridpoint 4.

It is also significant that the model correctly predicted both an early quasi-transition, and the actual spring transition at gridpoint 4, but that it missed the actual transition time at gridpoint 13 by about 4 weeks. This is consistent with the model tendency to shallow too much in this area. Long-term temperature comparisons in Figures 15 and 16 indicate no bias over most of the track. Model predictions at gridpoint 4, shown in Fig. 16, are very close to the actual profiles throughout the year. The actual temperatures at this gridpoint are similar to climatology, which is consistent with the occurrence of spring transition at the usual time. The long-term actual profiles appear to show above average temperatures for gridpoint 13, especially during the late summer through fall period, which corresponds to the earlier than normal spring transition in that area, as described in Elsberry and Garwood (1978). Model predictions for this gridpoint show general agreement with the actual temperatures, with a slight cold bias in the late summer and fall period.

B. SHORT-TERM RESULTS

1. Mixed Layer Depth

Bias and RMS error results were closely examined for the 15- and 30-day periods, and the results for the 60-day period were summarized. Contours of 15-day mixed layer depth bias for persistence and the average model are given in Figures 17 and 18, respectively. Errors are plotted at the time for which each 15-day prediction was initialized. Dashed contours indicate that the mixed layer depth prediction was shallower than the actual mixed layer depth. Examination of persistence errors

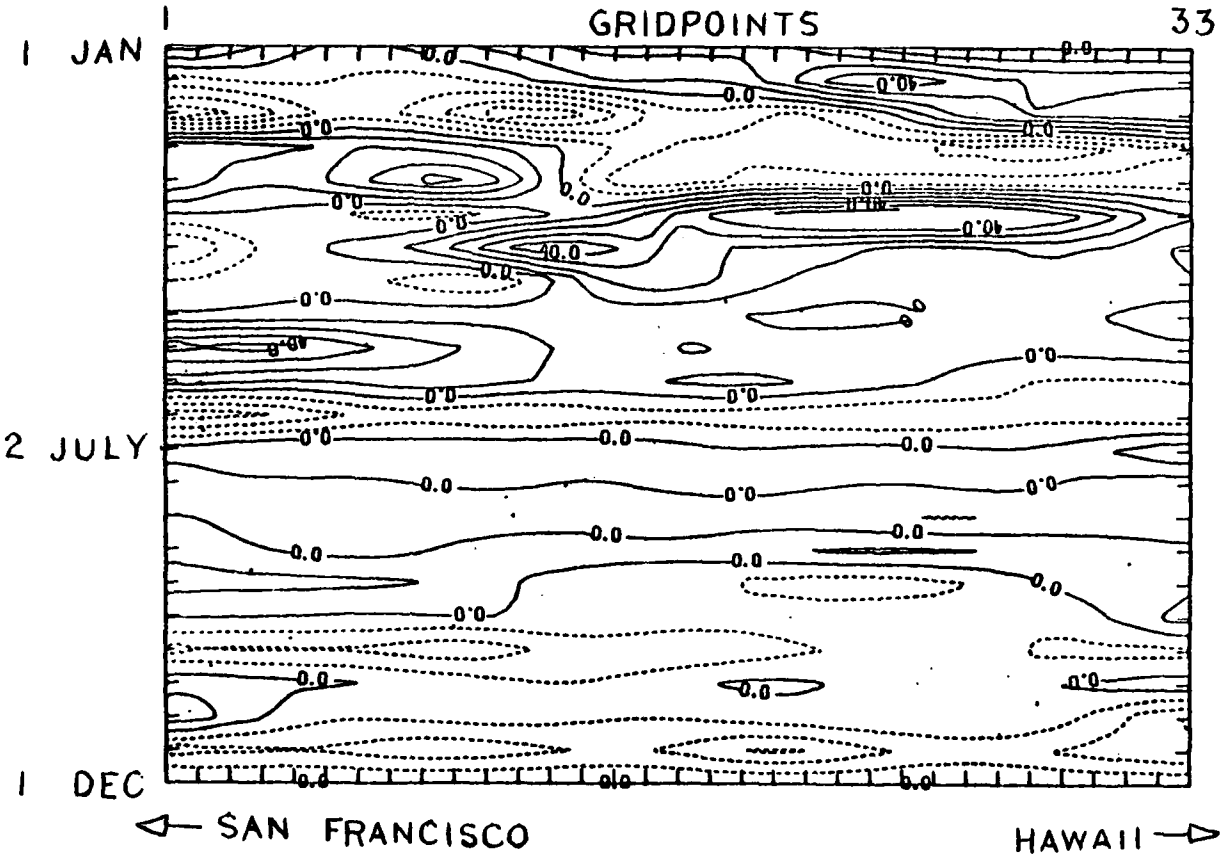

Fig. 17. Mixed Layer Depth errors (M) for a forecast of persistence between each 15-day time interval during the period 1 January 1978 through 1 December 1978. Values are plotted at the beginning of each 15-day forecast interval. Contour interval is 10 M. Dashed lines indicate values shallower than the actual mixed layer depths.

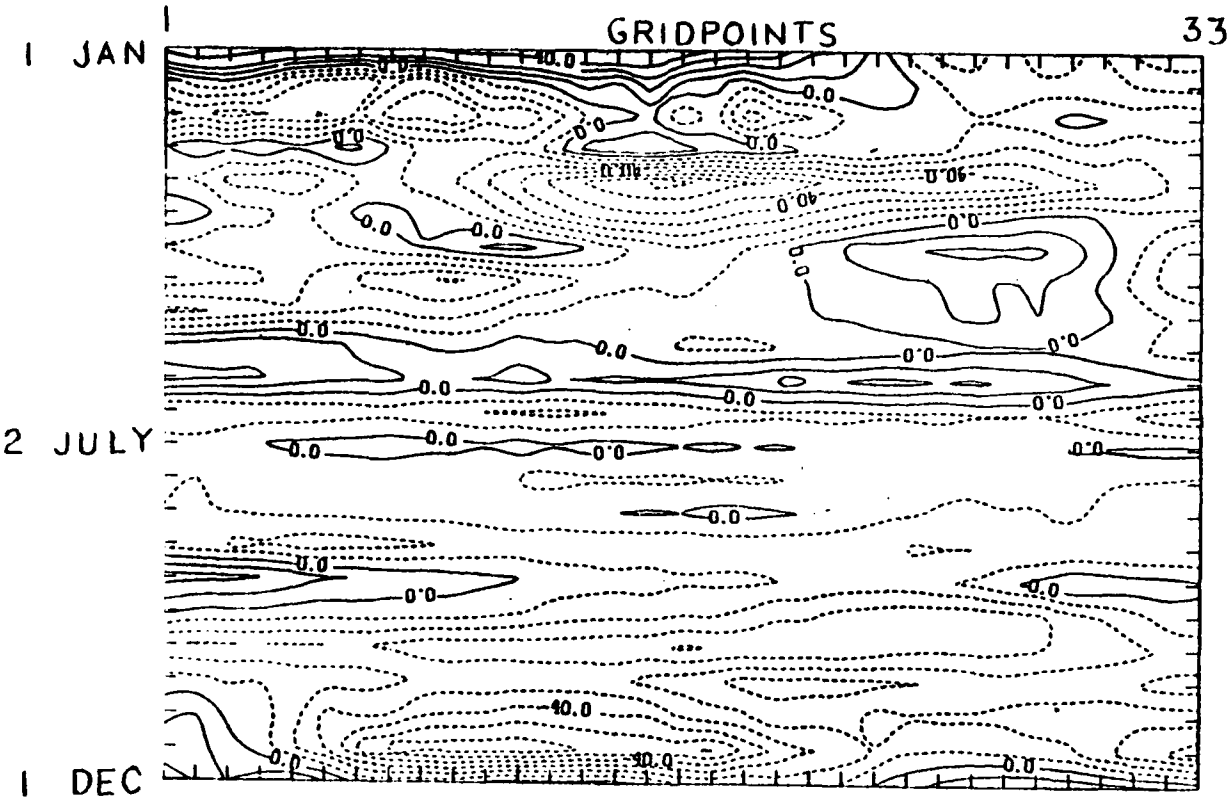

Fig. 18. Similar to Fig. 17, except for Average Model errors during each 15-day interval.

gives an indication of the annual cycle of changing mixed layer depth, and of the periods with significant changes that are of most interest in evaluating the model predictions.

The period from 1 January to 2 March was a period of relatively deep mixed layers on the average, with rapid changes occurring on a diurnal basis as the spring transition approached. Overall, the persistence error was low during this time period, with a marked difference in error along the track (Fig. 17). A deepening trend developed initially in the northern area, causing a negative persistence bias during this time period, while a shallowing trend in the south caused a positive bias. The model initially showed a positive bias over the northern part of the track and then a negative bias over the entire track (Fig. 18).

The early part of the period from 2 March to 2 May showed a relatively small negative error for persistence. As indicated in Fig. 17, rapid shallowing associated with the spring transition occurred in early March for the northern part of the track and in the middle of March for the southern part. Persistence showed a positive bias over the whole track for these two months, but the values were very close to zero after the rapid shallowing occurred. Corresponding model results (Fig. 18) indicate a large negative bias in the middle of the track where the model overpredicted the rapid shallowing event. There was a small negative bias elsewhere, indicating that the model-predicted mixed layer depth was too shallow.

The period 2 May to 1 September was a period of relatively little change in mixed layer depth, as noted by the near-zero values of

persistence error. An exception is noted during late June and early July near the northern boundary (Fig. 17). A period of shallowing (positive persistence error) is followed by a period of deepening. Model performance was similar to persistence. It is difficult to evaluate the actual performance of the model during this period, as the average mixed layer depth error was essentially the same magnitude as the expected observation error for the buoys.

The period 1 September to 1 December marked the period of the fall deepening as the mixed layer depth increased to larger winter values. Persistence errors (Fig. 17) were generally negative but small, reflecting the steady increase in mixed layer depth over the period. Model errors were consistently negative, indicating the consistent failure of the model to deepen sufficiently. In general, the model appeared to perform well during the summer period of little mixed layer depth change, and relatively well during the spring period of rapid mixed layer depth shallowing. It performed relatively poorly during the fall deepening period.

An examination of Figures 17 and 18 revealed areas with common error characteristics. Subarea 1, including gridpoints 1-7, is the region of the California Current, extending to the edge of the Subtropical Front. Persistence errors for this subarea, as shown in Fig. 17, indicate very little change from those discussed for the entire track. Errors were generally largest during the late winter through spring. Model results in this subarea indicate large errors during the fall through winter deepening period, but show relatively high accuracy throughout spring and summer. It is surprising that

these results tend to follow the pattern for the whole track, and that the errors are not larger, because this was expected to be a region of large advective effects.

Subarea 2 (gridpoints 8-19) is the transition region between the California Current and the warm subtropical water to the south. It extends three degrees latitude south of the Subtropical Front. Persistence errors (Fig. 17) were consistent with the overall trend of large errors during winter and spring, and relatively small errors for the remainder of the year. However, an examination of Fig. 18 reveals that this subarea consistently had larger model errors than did the rest of the track. The large negative bias indicated that the model mixed layer depths were substantially shallower than the actual mixed layer depths. It is possible that cold advection of modified subarctic water by the California Current is occurring in this region. Since the original heat budget performed for the entire track did not take this into account, an excessively large correction of downward heat flux may have been added to the total heat flux field in this subarea.

The third subarea (gridpoints 20-33) extends from the southern edge of the transition region to the southern end of the track. Persistence errors for this region appear to be similar to those for the other subareas. However, there is a substantial reduction in model error over the entire year, including a much smaller negative bias. It appears that the influence of the mixing and processes associated with the Subtropical Front have a well-defined range of influence. Because the track makes a 30 degree angle to the basically east-west front, the influence of the front is felt a full three degrees latitude

beyond the center of the front. Model errors (Fig. 18) decrease as the region of the homogeneous water mass of the Central North Pacific is approached.

Another comparison of the large error differences between the southern part of the track and the transition region can be seen in Figures 19 and 20, which are two-week mixed layer depth errors for gridpoints 13 and 30, respectively. Gridpoint 30 is representative of an area from gridpoints 20-33 in which the model did relatively well for both mixed layer depth and mixed layer temperature prediction. The error values for each successive two-week interval are given for persistence, climatology and the average model. The model error for gridpoint 13 can clearly be seen to have a large negative (too shallow) bias, while persistence and climatology appear to have little overall bias. The large positive climatology errors during the spring indicate that the actual profiles were much shallower than normal, which is consistent with the early spring transition previously noted. Gridpoint 30 results in Fig. 20 show that the model had a slight overall negative bias, while persistence and climatology again appear to have little bias. The lack of any large climatology errors indicates that gridpoint 30 experienced fairly typical mixed layer depths throughout the year. Climatology errors for gridpoint 30 appeared to be comparable in magnitude to those for persistence and the model predictions, but climatology error values for gridpoint 13 show erratic changes in sign. By summing over all gridpoints for the entire year, an overall bias of -10.2 M was obtained for the average model results. This indicated the tendency toward shallow mixed layer depths.

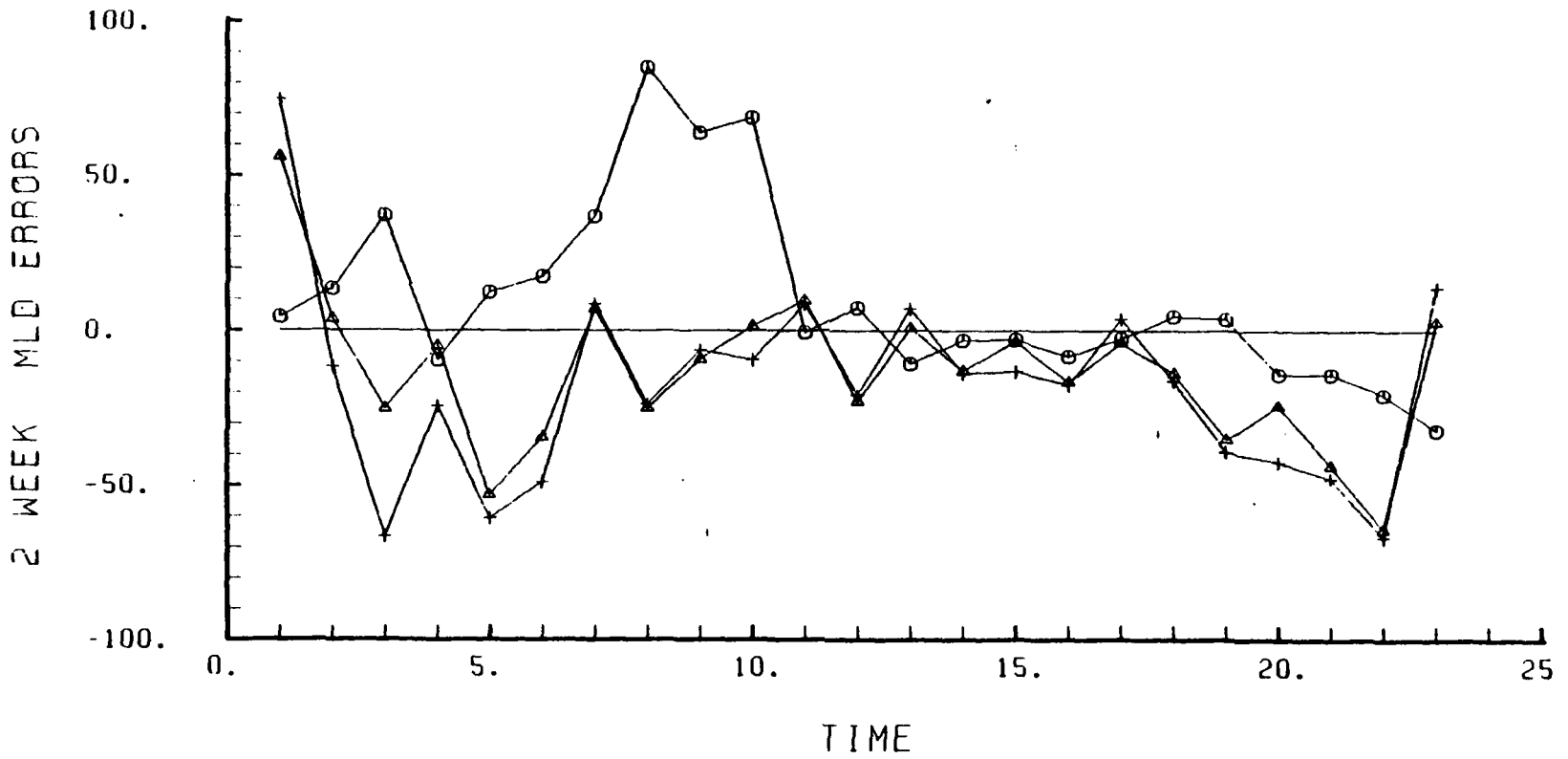

Fig. 19. 15-day Mixed Layer Depth errors (M) plotted at 15-day intervals, at gridpoint 13 for: Climatology = O , Persistence = + , Model = △ (time 1 = 1 Jan. 1978).

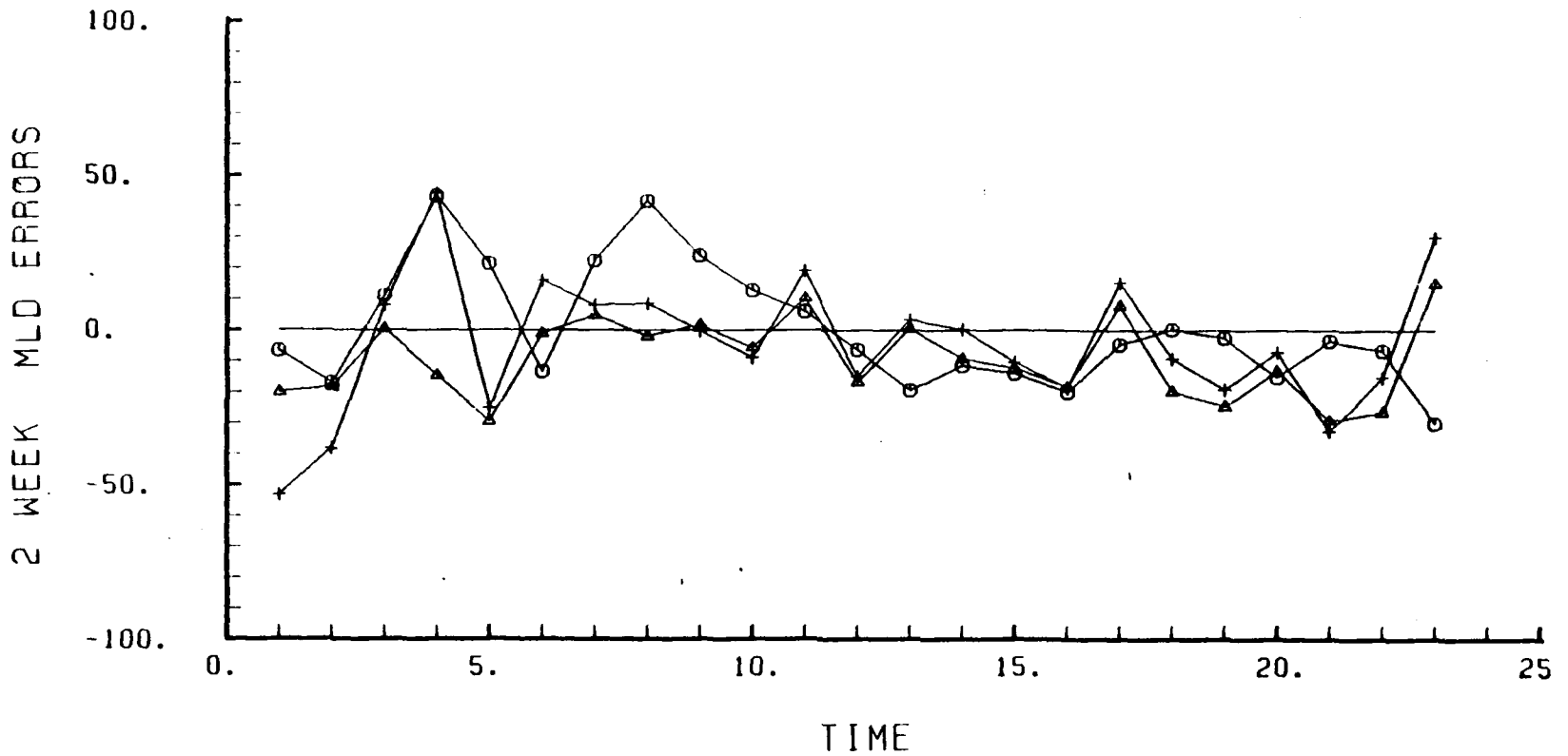

Fig. 20. Similar to Fig. 19, except at gridpoint 30.

Compared to persistence, the model performance improved at every gridpoint as the predictions were extended beyond the 15-day period. Contours of 30-day mixed layer depth errors for persistence and the model are shown in Figures 21 and 22, respectively. A comparison of Figures 17 and 21 reveals the large increase in error from 15-30 days for persistence. This increased error is present over most of the area, especially during winter and spring. By contrast, the relatively unchanged model error fields at 30 days (Fig. 22) are quite similar to the 15-day errors (Fig. 18).

An overall summary of RMS mixed layer depth error is shown in Figure 23. This summary includes results for all gridpoints over the entire year. The three types of model runs showed the expected pattern: Daily maximum depth profiles produced the best prediction, and the instantaneous profiles produced the worst. This is primarily because instantaneous observations of mixed layer depth were not available to verify rapid diurnal changes. The analyzed profiles were obtained using many observations, and any daily extremes were smoothed out, while the instantaneous profiles had an equal likelihood of occurring during any part of the diurnal cycle. The average model generated profiles had the advantage of smoothing out the extreme values of the diurnal cycle and were expected to perform better than the instantaneous profiles. Use of the daily maximum depth profiles was expected to provide the best prediction because it excluded the possibility of averaging extremely shallow model-generated mixed layer depths. Two of the model runs are superior to persistence and climatology after 25 days, while the daily maximum profile model is the best predictor over

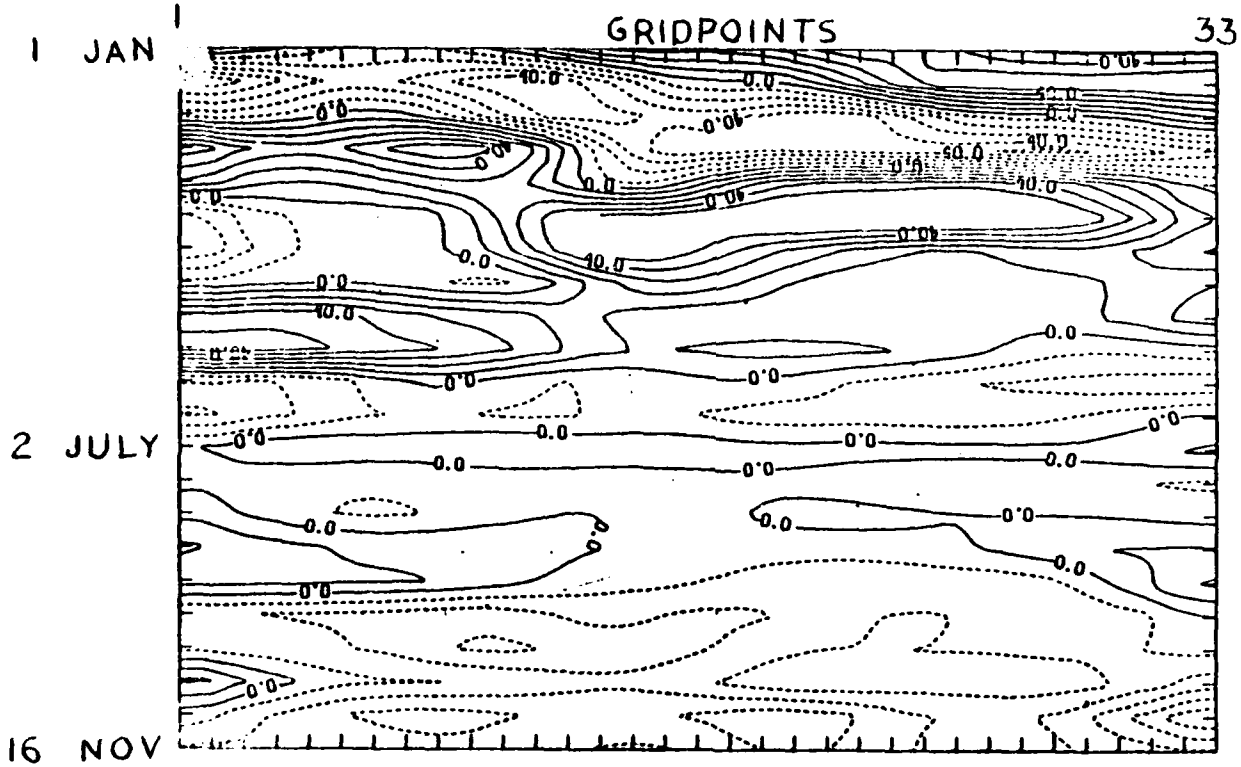

Fig. 21. Similar to Fig. 17, except for 30-day errors for the period 1 January - 16 November 1978.

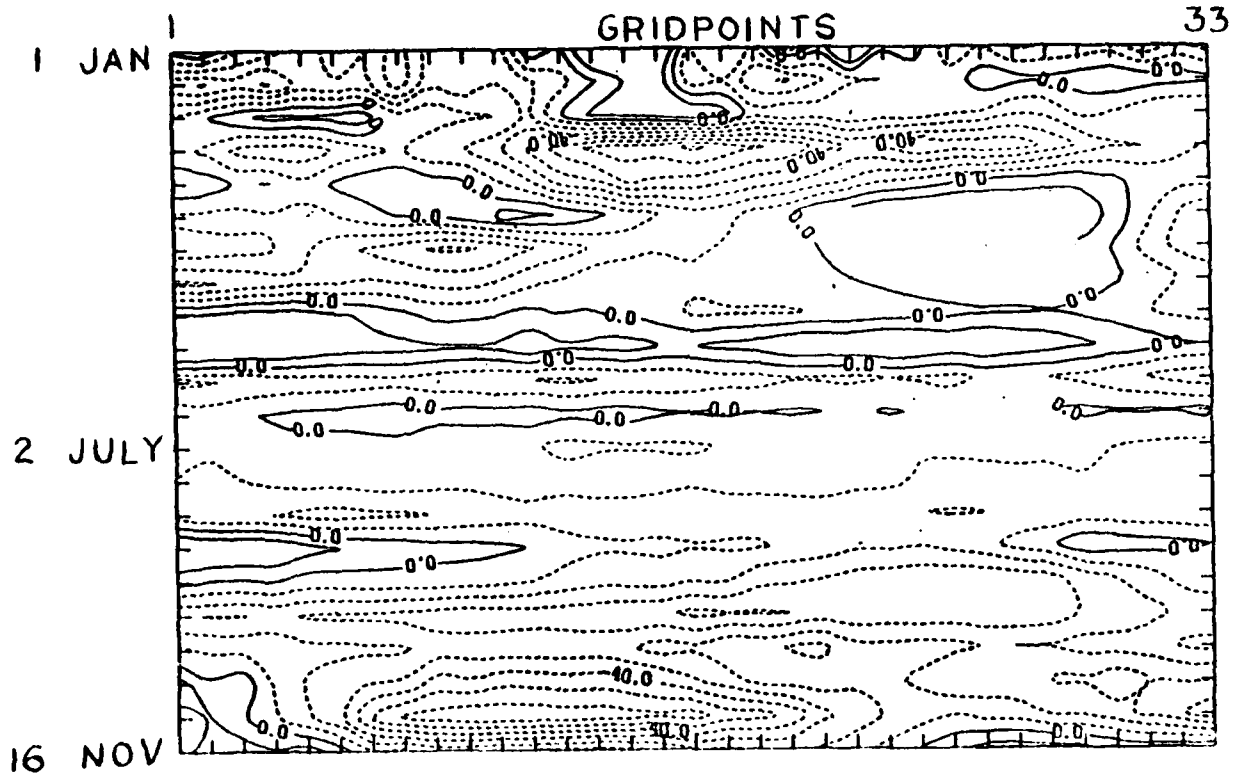

Fig. 22. Similar to Fig. 18, except for 30-day errors for the period 1 January - 16 November 1978.

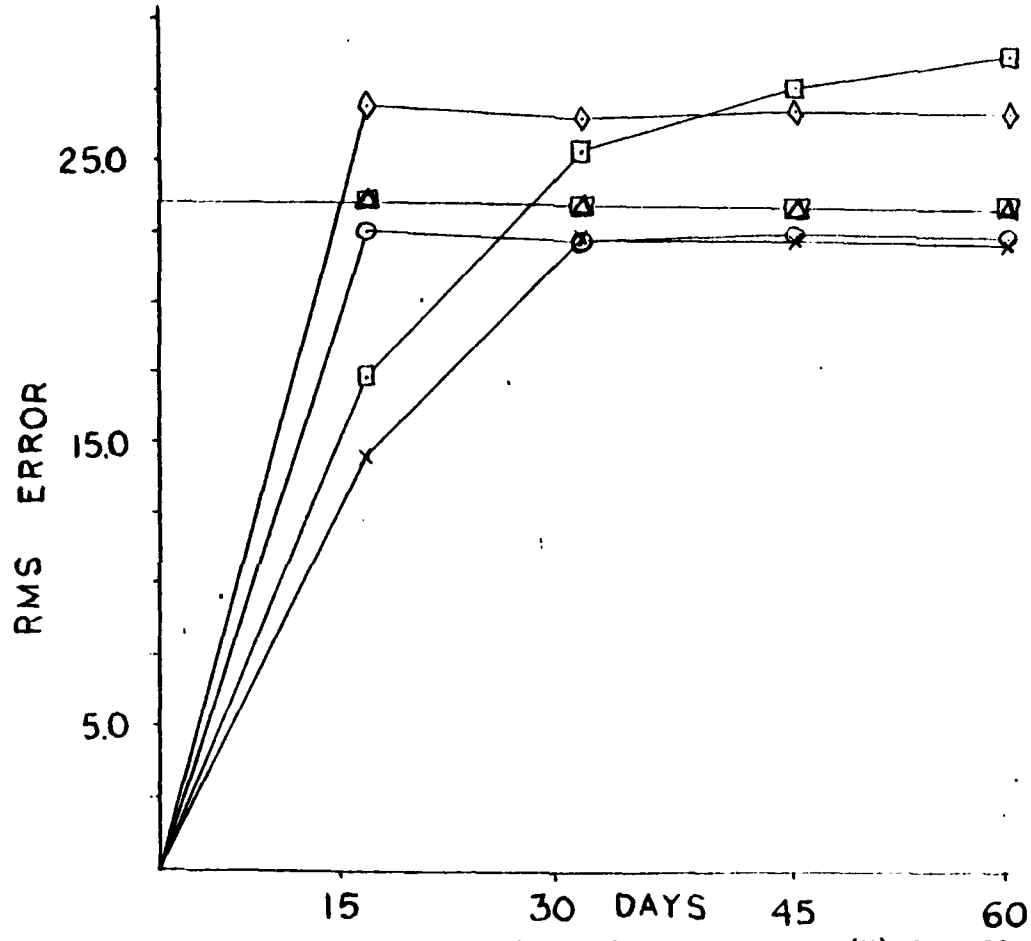

Fig. 23. Summary of 60-day RMS Mixed Layer Depth forecast errors (M) for all gridpoints over the entire year for: climatology (△), persistence (□), model instantaneous (◇), model cumulative average over 168 hours (○), model average of maximum daily mixed layer depths over 168 hours (x).

tne entire 60-day period. Separate RMS summaries for the three subareas (Table 1) inaicate that the model is clearly superior in the southern part of the track to 60 days. The predictions in the two northern parts of the track show the model results reaching the zero skill level after 10-15 days.

2. Sea-Surface Temperature

Contours of 15-day sea surface temperature errors for persistence and the average model are given in Figures 24 and 25, respectively. Dashed contours indicate that predicted sea surface temperature was lower than the actual sea surface temperature.

TABLE 1

RMS Mixed Layer Depth (M) Error
Summary for Subareas 1-3

RMS Error for:	15-Day	30-Day	45-Day	60-Day
Subarea 1				
Persistence	17.13	24.37	24.16	22.63
Climatology	15.46	15.46	15.46	15.46
Instantaneous	23.76	21.23	20.67	17.23
Average	20.63	18.16	18.10	16.92
Daily Max	14.57	18.51	18.03	16.83
Subarea 2				
Persistence	16.40	24.57	29.27	33.10
Climatology	27.74	27.74	27.74	27.74
Instantaneous	32.20	31.39	30.99	29.12
Average	26.97	25.92	26.86	26.12
Daily Max	15.76	24.88	26.79	26.06
Subarea 3				
Persistence	18.83	27.77	29.05	28.42
Climatology	24.53	24.53	24.53	24.53
Instantaneous	22.28	25.10	25.57	27.09
Average	19.48	19.96	20.67	20.81
Daily Max	16.24	20.02	20.55	20.75

During the period 1 January - 2 March, there was a slight decrease in sea surface temperature, which is reflected in the small

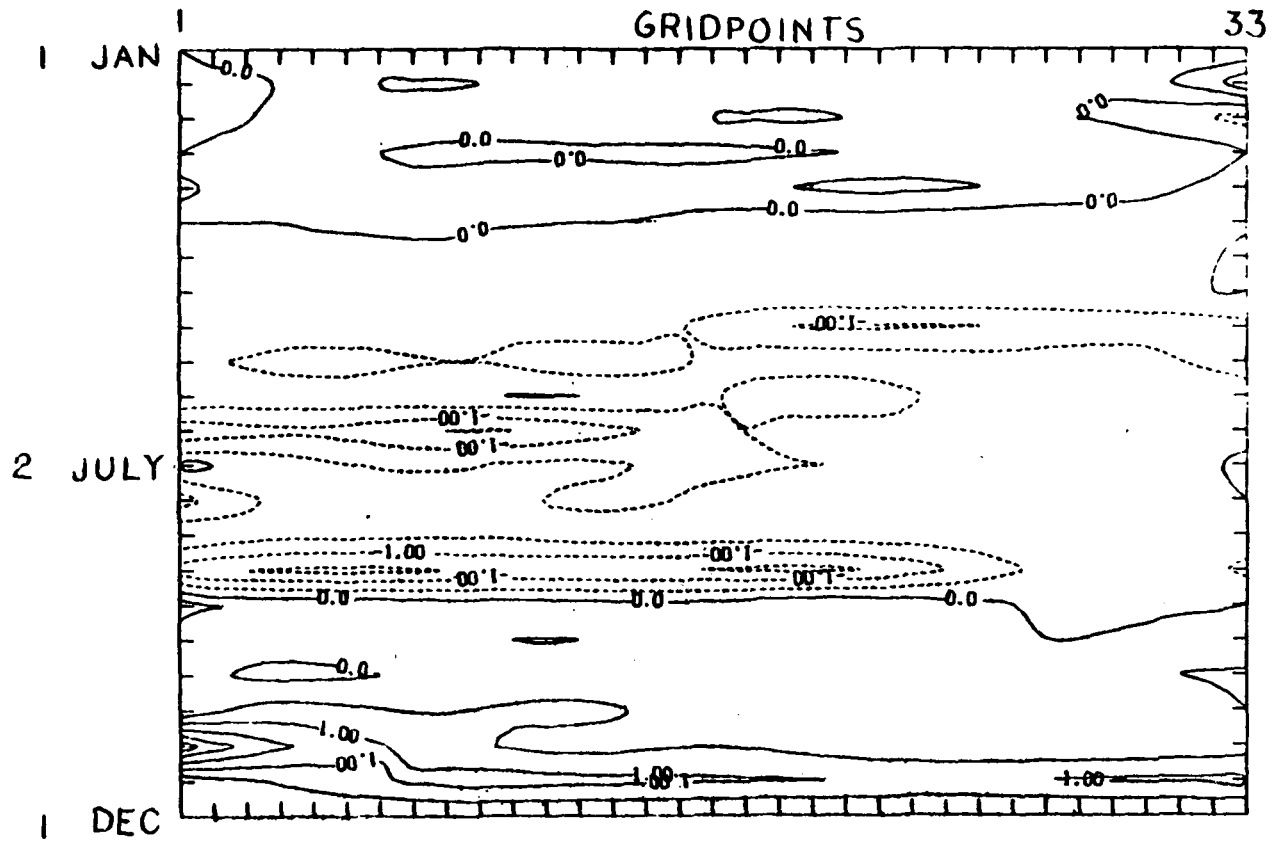

Fig. 24. Sea Surface Temperature ($\hat{t}$) error for persistence between each two-week interval during the period 1 January through 1 December 1978. Values are plotted at the beginning of each 15-day forecast interval. Contour interval is 0.5°C, Dashed lines indicate values lower than actual sea surface temperature.

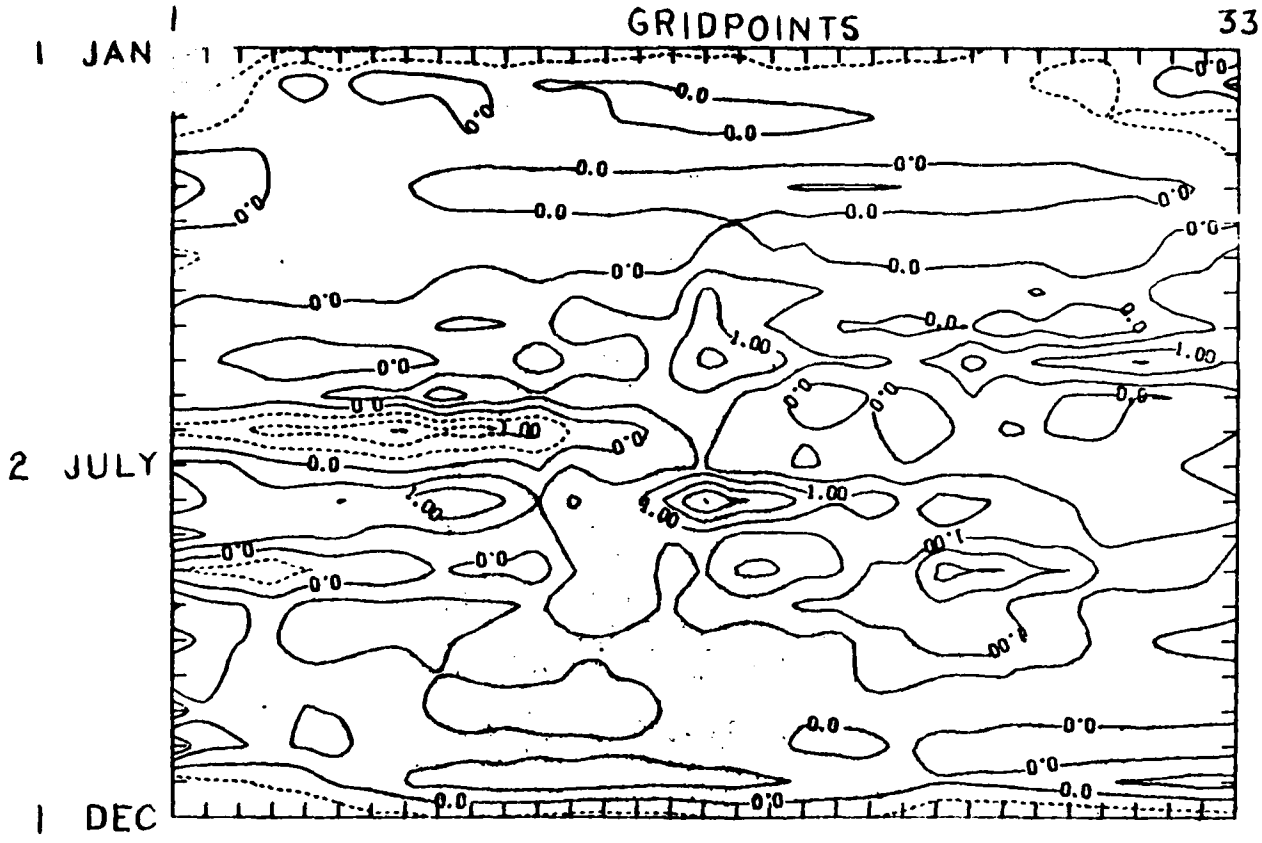

Fig. 25. Similar to Fig. 24, except for Average Model errors during each 15-day interval.

positive errors for persistence (Fig. 24). The model tended to underforecast the decrease in sea surface temperature as indicated by the slight positive bias (Fig. 25). This positive bias was characteristic of the model performance throughout the year over most of the track.

The period 2 March - 2 May can be seen to have very little persistence error (Fig. 24), while the model tended to overpredict the warming during this period (Fig. 25). The period 2 May - 1 August was one of relatively steady warming, following the spring transition. A negative error was found for persistence throughout the track. The model again overpredicted the temperature increases, and a positive bias was generally found. An exception to this trend was the underestimate of the warming during the first two weeks of June in the northern area (Gridpoints 1-14).

The period from 1 August - 1 September was marked by a rapid increase in sea-surface temperature, especially between gridpoints 1-25. A large negative bias is indicated over much of the track for persistence (Fig. 24). The model appears to have slightly overpredicted the increase, although it did relatively well compared to persistence. During 1 September - 1 November, a slight decrease in sea-surface temperature occurred as the layer deepened. Persistence errors were now slightly positive. The model predictions during this period were also good, with only a slight positive bias over central and southern portions of the track. Finally, the period from 1 November - 1 December was marked by a large sea surface temperature decrease. This decrease is indicated by large positive errors for persistence (Fig. 24). The model did a relatively good job of predicting this change, as rather small errors are indicated in Figure 25 during this period.

In general, the accuracy of the model-predicted sea surface temperature was comparable to persistence. A tendency for predicting sea-surface temperatures too high was observed throughout the track. Because of this bias, the model had smaller errors during warming than during cooling periods.

An examination of Figures 24 and 25 indicates that the persistence errors tend to have a uniform sign along the entire track. The northern part of the track shows slightly larger errors due to a more rapid heating and cooling process occurring in that region. The model temperature errors have less coherence along the track, with generally larger errors to the north. The model predictions in the transition region appear to have the largest positive errors throughout the entire year, while large positive errors in the region of the California Current are concentrated in the summer. Several areas of large sea surface temperature errors are noted, including one at the northern part of the track in June and one in the central part of the track in July.

A comparison of error differences between subareas 2 and 3 can be seen in Figures 26 and 27, which are two-week sea-surface temperature errors for gridpoints 13 and 30, respectively. There is a large positive temperature bias at gridpoint 13 from April through December in the model. Each of the two-week model runs is independent. Nevertheless, frequently there are positive errors exceeding 0.5°C in each two-week period. For most of this summer warming season, persistence shows a negative bias. Climatology shows the expected negative bias at gridpoint 13 for the period following the early spring transition,

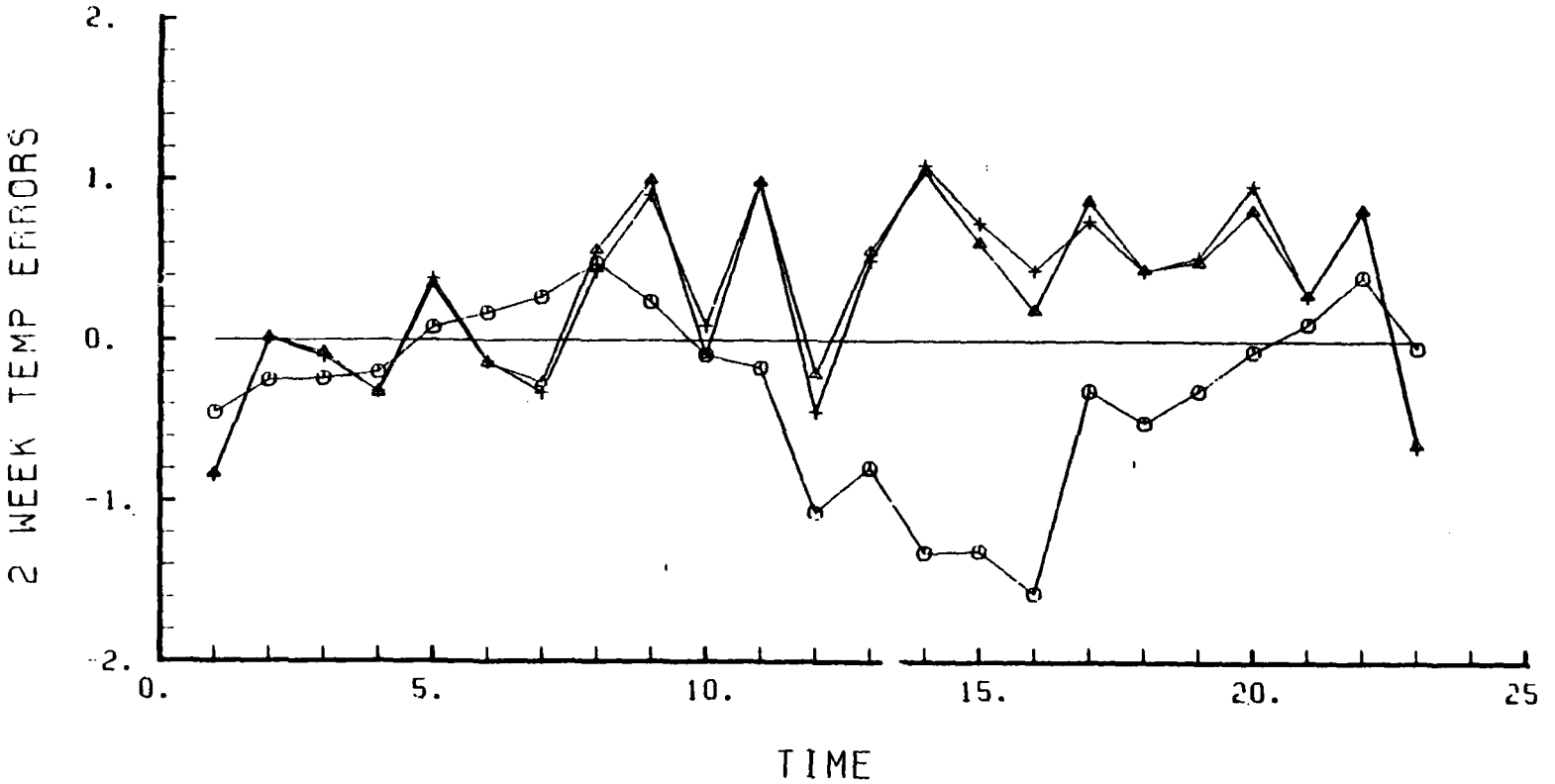

Fig. 26. Similar to Fig. 19, except for Sea Surface Temperature errors (°C).

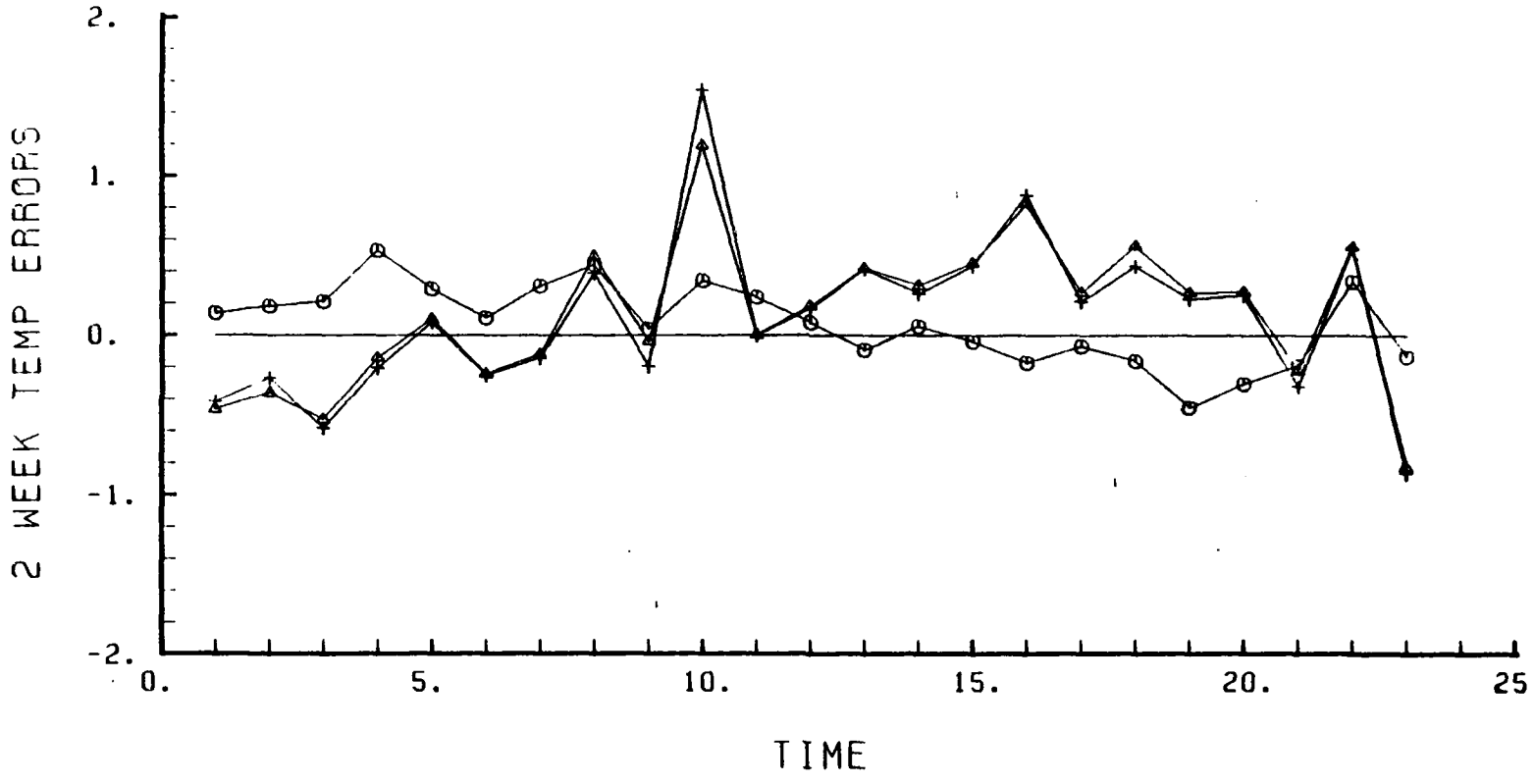

Fig. 27. Similar to Fig. 26, except for gridpoint 30.

indicating that the actual sea surface temperatures are warmer than climatology. Model errors for gridpoint 30 (Fig. 27) indicate little bias over the entire year, but show large fluctuations. A similar fluctuation pattern is indicated by the persistence errors. There is no apparent bias in the climatology errors for gridpoint 30, which is consistent with the normal spring transition which occurred at that point.

By summing over all gridpoints for the entire year, an overall RMS sea-surface temperature error of .59°C was observed for the average model run, compared to .53°C for persistence. An overall positive bias for the model indicated that model temperatures were higher than the actual sea-surface temperatures. Contours of 30-day sea surface temperature errors for persistence and the average model are given in Figures 28 and 29, respectively. A comparison of Figure 24 and 28, and Figure 25 and 29, shows that the model error from 15-30 days increases at the same rate as the persistence error, and that the temperature errors for each of the fields tend to increase relatively uniformly over the entire track for the entire year.

An overall summary of RMS sea-surface temperature error is shown in Figure 30. The daily maximum model-predicted profiles and persistence appear to have similar accuracy, and these two are superior to climatology to about 23 days. All of the predictors except climatology are approximately the same beyond 40 days. Separate RMS summaries for the three subareas (Table 2) indicate that the model is the best predictor out to 40 days for subarea three, except for the region of gridpoint 25. The model is superior to 20 days for subarea 1, and reaches the zero skill level at approximately 8 days in subarea 2.

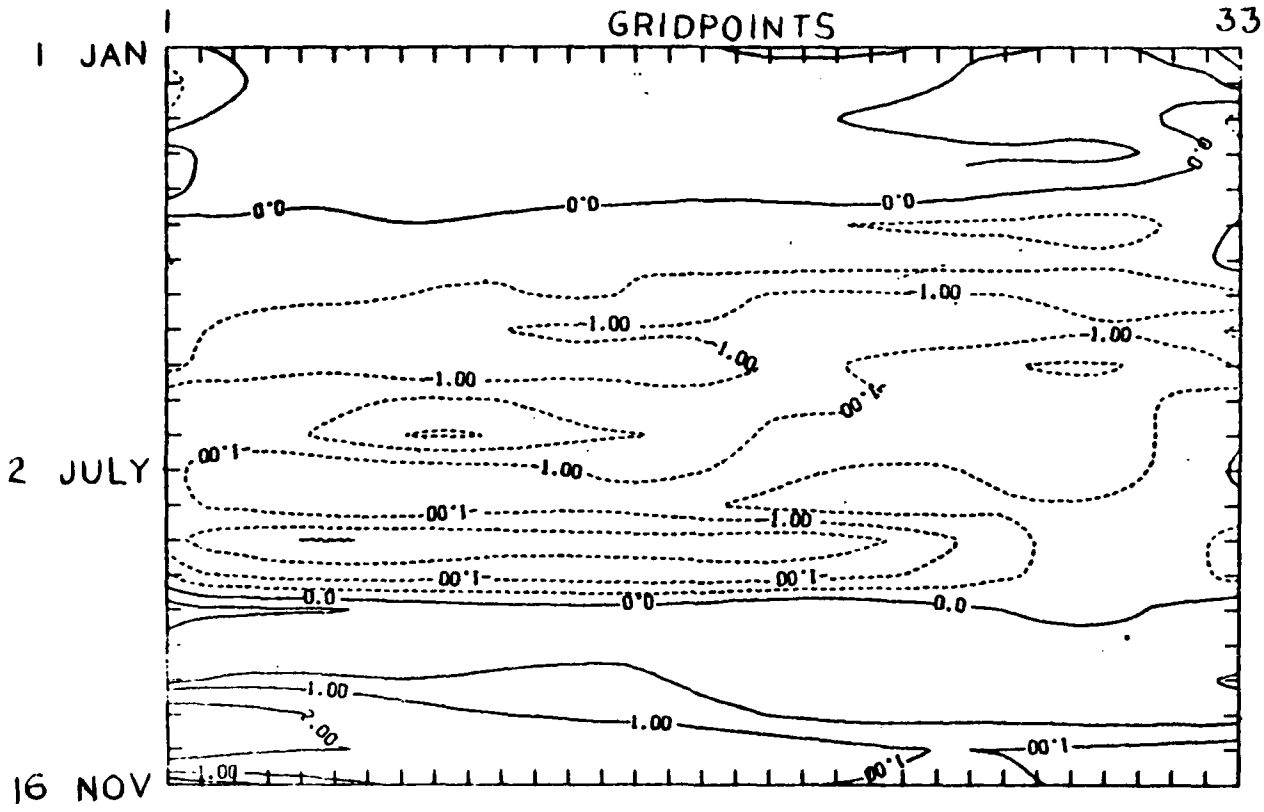

Fig. 28. Similar to Fig. 24, except for 30-day error for the period 1 January - 16 November 1978.

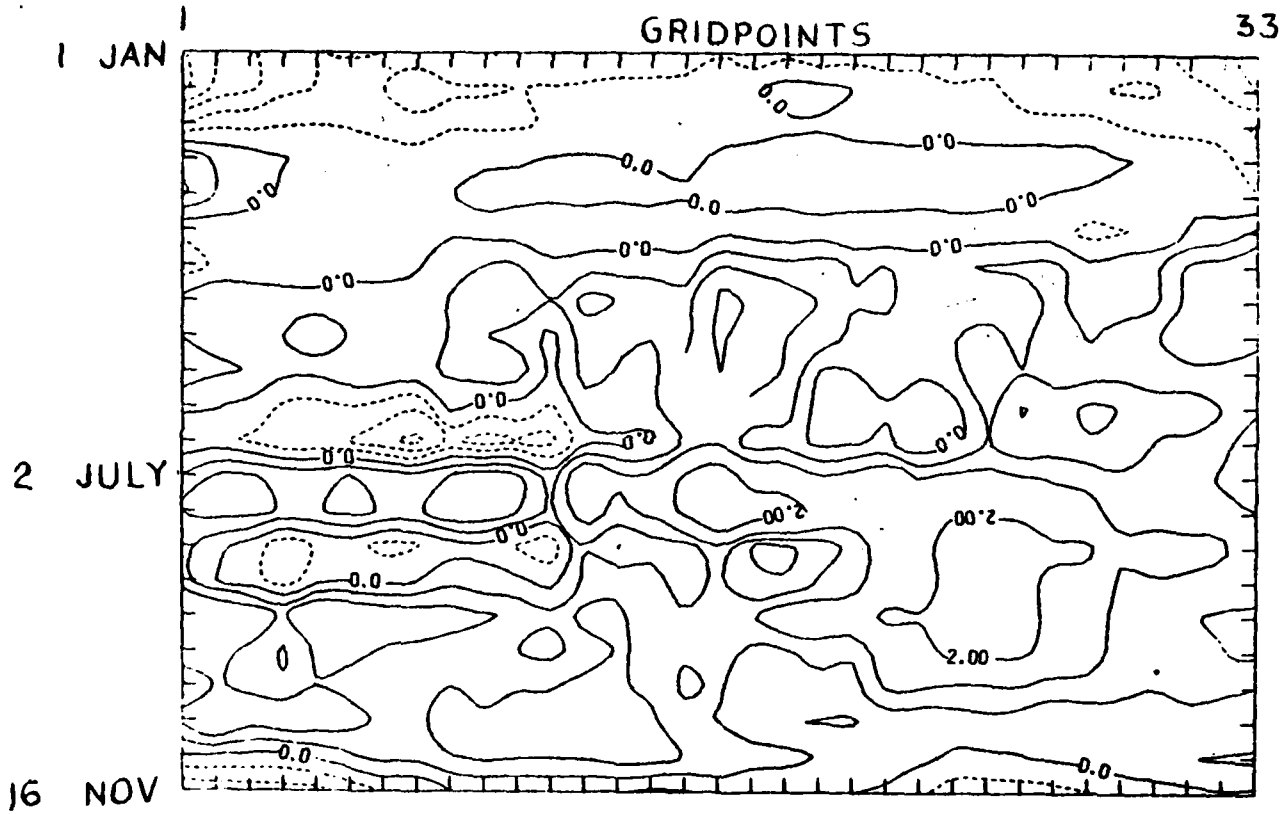

Fig. 29. Similar to Fig. 25, except for 30-day error for the period 1 January - 16 November 1978.

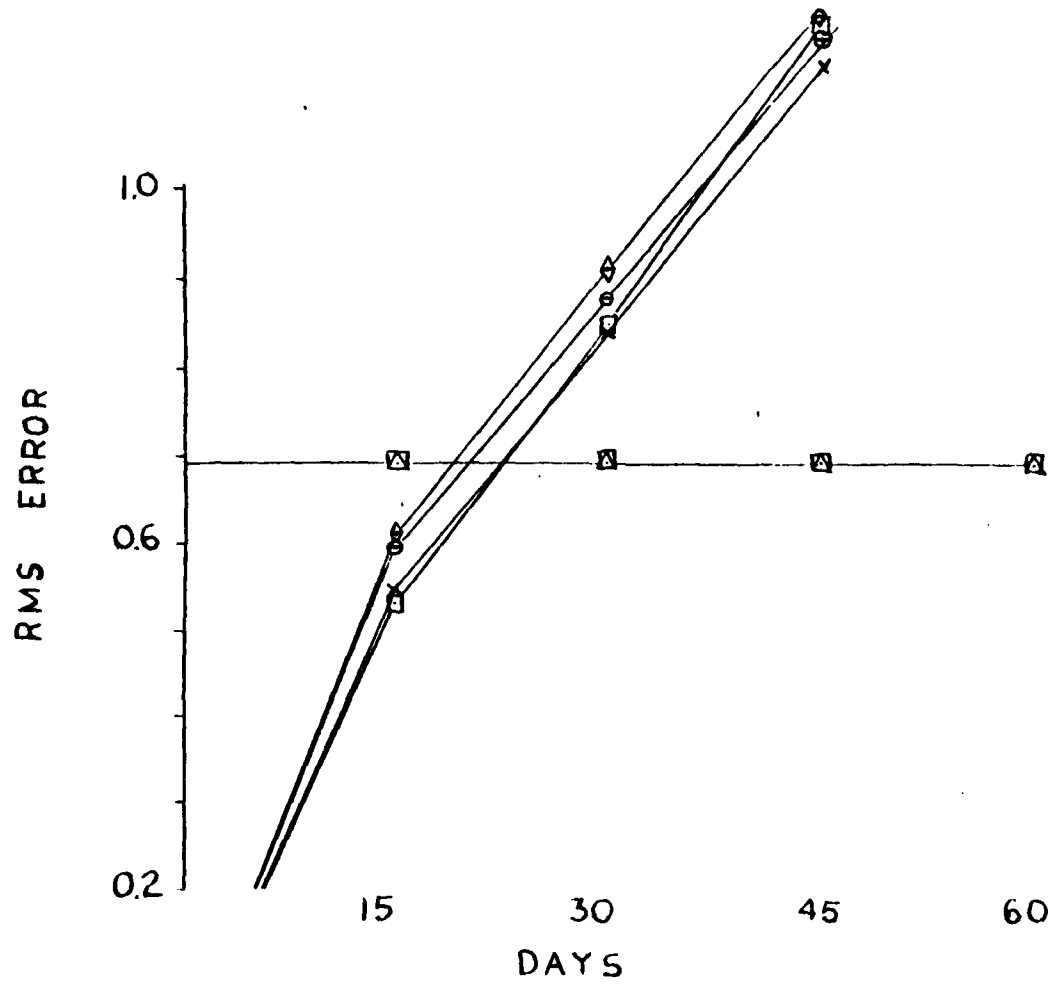

Fig. 30. Similar to Fig. 23, except for Sea Surface Temperature error (°C).

TABLE 2

RMS Sea-Surface Temperature (°C)
Error Summary for Subareas 1-3

RMS Error for:	15-Day	30-Day	45-Day	60-Day
Subarea 1				
Persistence	0.56	0.93	1.29	1.63
Climatology	0.79	0.79	0.79	0.79
Instantaneous	0.62	0.88	1.18	1.42
Average	0.59	0.85	1.13	1.38
Daily Max	0.56	0.82	1.08	1.34
Subarea 2				
Persistence	0.42	0.66	0.84	0.99
Climatology	0.36	0.36	0.36	0.36
Instantaneous	0.56	0.81	1.09	1.34
Average	0.54	0.79	1.07	1.32
Daily Max	0.48	0.69	0.98	1.30
Subarea 3				
Persistence	0.64	1.03	1.40	1.69
Climatology	0.93	0.93	0.93	0.93
Instantaneous	0.63	0.93	1.08	1.15
Average	0.62	0.88	1.06	1.16
Daily Max	0.59	0.85	1.02	1.13

VI. CONCLUSIONS

The model was shown to perform in a highly competitive manner when compared to other methods in the prediction period to 60 days for mixed layer depth, and to 23 days for sea surface temperature. There was a marked difference in the performance of the model in different locations along the track between San Francisco and Hawaii. Areas where the predictions were poor seem to be regions where the basic model assumptions were invalid, and especially where advective or diffusive effects are expected to be important. The 15-day model results are clearly better than a persistence forecast only when the model predictions at times of daily maximum mixed layer depth were used. The use of this model for predictions verified by a 15-day analyzed field requires a model output that will exclude the diurnal oscillations. It appears that this was only accomplished using the daily maximum layer depth predictions.

A bias in the model resulted in too-shallow mixed layer depths and too-high mixed layer temperature. This problem was analyzed by examining the model results over specific periods of time, and in specific locations along the track. The performance of the model in each of the subareas for space and time indicated a common tendency. It appeared that the net upward heat fluxes were too small. This excessive downward heat flux tended to prevent rapid deepening and cooling of the upper ocean. Conversely, the periods of shallowing

and warming of the near-surface layers were overpredicted. This apparent bias in the model caused its performance to vary greatly over the annual sequence of changes in the mixed layer depth and sea-surface temperature.

There are several possible causes for this bias in the model. The specified correction to the total heat flux may have been too large. It appears that this was the case in the vicinity of the transition region, where the entire difference between change in oceanic heat content and uncorrected total heat flux was attributed to error in the total heat flux field. The existence of horizontal advective processes of relatively large magnitude in this region may have invalidated the assumption of a balance of heat due solely to vertical processes. However, the local heat balance assumption should still be valid over much of the track. Nevertheless, an overall bias in mixed layer depth of approximately -10 M was obtained. There are several other factors which can be considered. The total heat flux was adjusted to a smoothed change in heat content field during 1978, which may have actually contained some transient features of large magnitude. If this were the case, then it is likely that these features included both positive and negative deviations from the smoothed field. Consequently, an alternation between negative and positive mixed layer depth errors might have been expected. The fact that the bias was consistently negative reduces the possibility that the transient features were the major problem. Another factor which must be considered is the data base used to determine the objectively analyzed profiles on the time-space grid. The average number of bathythermograph buoys considered

during each time period was approximately 80. However, the minimum number was 37. During this time period, the number of BTs applied for the weighted correction at any one gridpoint was approximately six. So it is possible that there is a bias in the values of the profiles used to initialize and verify the model runs at a few times of the year. The question of how much this affected the overall results can best be answered by further study in this same area, considering other years, especially those in which the sampling size was considerably larger for the times of low data density of this study.

Another factor which must be considered is the effect on the results due to the method in which the mixed layer depth was defined. Redefining the model output profiles using the definition of the mixed layer depth which was used for the analyzed profiles, i.e. that depth at which the temperature profile changes from a relatively isothermal one, to one with a decrease in temperature exceeding 0.10°C in 5 M, results in a reversal of the mixed layer depth bias. It can be seen that the model-generated mixed layer depths tend to be shallower than those produced by an analysis which defines the mixed layer depth as the top of the major thermocline. Model generated transient isothermal layers near the ocean surface, which have a very small temperature jump at their base, can be interpreted to be the major isothermal layer which contains the large temperature gradient of the thermocline at its base. This problem of interpretation can be solved by the use of a consistent definition for the mixed layer depth, at least in areas which show a similar annual cycle.

Selection of the maximum mixed layer depth profiles in certain runs tended to stabilize the model results, which otherwise included these model generated shallow, transient isothermal layers. While these features may actually be present, they are not observed in the verifying profiles. This is due to the relatively large 15-day time interval, and to the objective analysis smoothing process. Ship wake generated turbulence in the area of expendable bathythermograph soundings may also eliminate these shallow layers by remixing down to the primary mixed layer depth, so the use of a prediction scheme which does not consider these features is especially recommended when ship-launched expendable bathythermograph buoys have been used. The alteration of the upper ocean thermal structure by the observing ships is not believed to be a major problem for this type of analysis, since the time resolution of the present data are inadequate to treat this point. It must be determined by other studies with much smaller time resolution if these features are important in the determination of an overall sound velocity structure with operational application.

The model results in this study include a negative mixed layer depth bias and a corresponding positive mixed layer temperature bias. Several possible factors have been examined which might have contributed to this problem, and the point has been made that a critical factor in the results is the method of determining the mixed layer depth. While it appears that the depth bias is primarily a result of interpretation of the mixed layer depth, the possibility must be considered that the model contains some parameterizations of physical processes that need improvement, and that, in its present form, the model contains an

internal bias. The best way to determine this is by comparison with other studies, in the same location, and in different locations. The use of actual BT profiles and a standard definition of the mixed layer depth is recommended. Operational use of the model in its present form, and in the location of this study, is not advisable until further studies have been performed. However, it must be remembered that the bias which was shown to exist had a varying effect over the annual cycle and along the track. The actual reliability of the model as the best available predictor of changes in the upper ocean temperature structure for certain subareas was noted. It is entirely consistent with the ideas outlined in Elsberry and Garwood (1979) that application of this model would show large variability in performance in different oceanic regimes, and that the use of this model as a "first-generation" mixed layer model can best be determined by continued research.

LIST OF REFERENCES

Budd, B. W., 1980: Prediction of the Spring Transition and Related Sea-Surface Temperature Anomalies. Master's Thesis, Naval Postgraduate School, Monterey, 95 pp.

Cressman, G. P., 1959: An Operational Objective Analysis System. Monthly Weather Review, 87(10), 367-374.

Dorman, C. E. and J. F. T. Saur, 1978: Temperature Anomalies Between San Francisco and Honolulu, 1966-1974, Gridded By an Objective Analysis. Journal of Physical Oceanography, 8(2), 247-257.

Elsberry, R. L., P. C. Gallacher, R. W. Garwood Jr., 1979,: One Dimensional Model Predictions of Temperature Anomalies During Fall 1976. Naval Postgraduate School Technical Report NPS 63-79-003, 30 pp.

Elsberry, R. L. and R. W. Garwood Jr., 1978: Sea-Surface Temperature Anomaly Generation in Relation to Atmospheric Storms. Bulletin of the American Meteorological Society, 59, 786-789.

Elsberry, R. L. and R. W. Garwood Jr., 1979: First-Generation Numerical Ocean Prediction Models - Goal for the 1980's. Naval Postgraduate School Technical Report NPS 63-79-007, 41 pp.

Gallacher, P. C., 1979: Preparation of Ocean Model Forcing Parameters From FNWC Atmospheric Analysis and Model Predictions. Naval Postgraduate School Technical Report NPS 63-79-005, 24 pp.

Garwood, R. W. Jr., 1977: An Oceanic Mixed Layer Model Capable of Simulating Cyclic States. Journal of Physical Oceanography, 7, 455-468.

Gill, A. E. and P. P. Niiler, 1973: The Theory of the Seasonal Variability in the Ocean. Deep-Sea Research, 20, 141-177.

Kraus, E. B. and J. S. Turner, 1967: A One Dimensional Model of the Seasonal Thermocline, II. The General Theory and Its Consequences. Tellus, 19, 98-106.

Saur, J. F. T., 1980: Surface Salinity and Temperature on the San Francisco - Honolulu Route June 1966 - December 1970 and January 1972 - December 1975. Journal of Physical Oceanography, 10(10), 1669-1680.

Saur J. F. T., L. E. Eber, D. R. McLain and C. E. Dorman, 1979: Vertical Section of Semimonthly Mean Temperature on the San Francisco - Honolulu Route: From Expendable Bathythermography Observations, June 1966 - December 1974. NOAA Technical Report NFMS SSRF-728, 35 pp.

Schnoor, R. T., 1975: Monthly Heat Budget Calculations for the Eastern North Pacific Ocean Using Synoptic-Scale Data. Master's Thesis, Naval Postgraduate School, Monterey, 66 pp.

Wyrtki, K. and K. Haberland, 1968: On the Redistribution of Heat in the North Pacific Ocean. Journal of the Oceanographical Society of Japan, 24(5), 220-233.

INITIAL DISTRIBUTION LIST

		No. Copies
1.	Defense Technical Information Center Cameron Station Alexandria, VA 22314	2
2.	Library, Code 0142 Naval Postgraduate School Monterey, Ca 93940	2
3.	Dr. R. J. Renard, Code 63Rd Chairman, Department of Meteorology Naval Postgraduate School Monterey, CA 93940	1
4.	Dr. C. N. K. Mooers, Code 68Mr Chairman, Department of Oceanography Naval Postgraduate School Monterey, CA 93940	1
5.	Dr. R. L. Elsberry, Code 63Es Department of Meteorology Naval Postgraduate School Monterey, CA 93940	5
6.	Dr. R. W. Garwood, Code 68Gd Department of Oceanography Naval Postgraduate School Monterey, CA 93940	1
7.	Mr. P. C. Gallacher, Code 63 Department of Meteorology Naval Postgraduate School Monterey, CA 93940	1
8.	Dr. D. R. McLain Pacific Environmental Group National Marine Fisheries Service Monterey, CA 93940	1
9.	Commanding Officer (Attn: S. Piacsek) Naval Ocean Research and Development Agency NSTL Station, MS 39529	1

10. Commander — 1
Naval Oceanography Command
NSTL Station, MS 39529

11. LT. E. F. Steiner, USN — 2
8440 57th Avenue
Berwyn Heights, MD 20740

12. Dr. R. L. Haney, Code 63Hy — 1
Department of Meteorology
Naval Postgraduate School
Monterey, CA 93940

13. Director — 1
Naval Oceanography Division
Navy Observatory
34th and Massachusetts Avenue NW
Washington, D.C. 20390

14. Commanding Officer — 1
Fleet Numerical Oceanography Center
Monterey, CA 93940

15. Commanding Officer — 1
Naval Environmental Prediction Research
Facility
Monterey, CA 93940

16. Chairman, Oceanography Department — 1
U.S. Naval Academy
Annapolis, MD 21402

17. Commanding Officer — 1
Naval Oceanographic Office
NSTL Station, MS 39529

18. LCDR C. Dunlap, Code 68Du — 1
Department of Oceanography
Naval Postgraduate School
Monterey, CA 93940

19. Dr. G. O. Williams — 1
Science Applications, Inc.
1200 Prospect St.
P.O. Box 2351
La Jolla, CA 92038